
Differentiation Through Black-Box Quadratic Programming Solvers

Connor W. Magoon¹, Fengyu Yang¹, Noam Aigerman², Shahar Z. Kovalsky¹

¹University of North Carolina at Chapel Hill, ²University of Montreal

Abstract

Differentiable optimization has attracted significant research interest, particularly for quadratic programming (QP). Existing approaches for differentiating the solution of a QP with respect to its defining parameters often rely on specific integrated solvers. This integration limits their applicability, including their use in neural network architectures and bi-level optimization tasks, restricting users to a narrow selection of solver choices. To address this limitation, we introduce **dQP**, a modular and solver-agnostic framework for plug-and-play differentiation of virtually any QP solver. Our key theoretical insight is that the solution and its derivative can each be expressed in terms of closely-related and simple linear systems by using the active set at the solution. This insight enables efficient decoupling of the QP’s solution, obtained by any solver, from its differentiation. Our open-source, minimal-overhead implementation will be made publicly available and seamlessly integrates with more than 15 state-of-the-art solvers. Comprehensive benchmark experiments demonstrate dQP’s robustness and scalability, particularly highlighting its advantages in large-scale sparse problems.

1 Introduction

Computational methods often rely on solving optimization problems, *i.e.*, finding an optimum of an objective function subject to constraints. This has led to the development of numerous high-performance open-source and commercial solvers, particularly for constrained convex optimization [114, 27]. Recently, there has been growing interest in *differentiable optimization*, which enables gradient-based learning through optimization layers that show promise across applications such as image classification [8], optimal transport [97, 98], zero-sum games [75], tessellation [35], control [9, 38, 40], decision-making [110], robotics [62], biology [116], and NLP [111].

Differentiable optimization focuses on computing the derivatives of the optimal solution to an optimization problem with respect to parameters defining the problem’s objective and constraints. Rooted in classical sensitivity analysis and parametric programming [99, 100, 47, 49, 48, 73, 26, 93], it has gained momentum through the idea that optimization problems can be embedded as parameterized “layers” within neural networks – training such layers requires computing the derivative (gradient) of the optimization problem’s solution during backpropagation [5, 1, 23].

This paper focuses on differentiating solutions to Quadratic Programs (QPs) – a core class of convex problems involving the minimization of a quadratic objective subject to linear inequality constraints.

Despite significant research efforts, existing approaches for differentiating QPs fail to fully leverage state-of-the-art solvers. General-purpose methods that support a broad class of optimization problems often include QPs, but they sacrifice efficiency and robustness for generality, underperforming compared to QP-specific methods. On the other hand, recent QP-specific approaches are tightly coupled with particular or proprietary solvers (*e.g.*, for batching small QPs), limiting their flexibility [5, 17, 29].

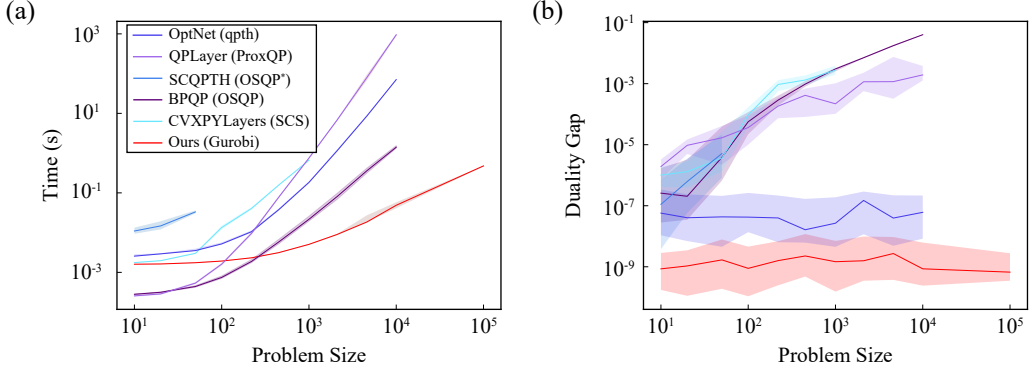


Figure 1: Comparison of differentiable QP methods for projection onto the probability simplex, evaluated by (a) solve time and (b) solution accuracy (duality gap). For moderately sized problems, our approach, using the Gurobi QP solver, outperforms existing methods on both metrics. As problem size increases, our method remains efficient, while others become intractable.

This tight integration restricts broader applicability. Solving QPs efficiently and reliably often requires advanced solvers like Gurobi [58] and MOSEK [10], developed over years of academic and commercial effort. These solvers handle scales and complexities that non-industrial implementations cannot. However, no single solver fits all problems, making solver choice critical. To our knowledge, no existing approach provides a robust, efficient, and fully flexible framework and implementation for differentiating QPs across solvers.

We introduce **dQP**, a modular, solver-agnostic framework that transforms any QP solver into a differentiable layer. Our key insight is that the gradient of a QP solution can be computed *explicitly* using the primal solution and the active set of constraints, both obtainable from the solver. Building on classical sensitivity theory, we show that the gradient can be expressed through a reduced linear system involving only the active constraints. Moreover, the active set can be used not only to simplify the gradient computation but also to easily recover the dual solution if not returned by the solver.

We implement dQP as an open-source, minimal-overhead layer on top of `qpsolvers` [32], enabling seamless integration with over 15 commercial and free solvers, and straightforward extension to additional ones. Our modular approach allows users to select the best solver for their task while providing differentiability. We evaluate dQP on a benchmark of over 2,000 diverse QPs and demonstrate superior performance compared to existing methods, particularly in large-scale structured sparse problems, as demonstrated in Figure 1.

Our contributions:

1. We prove that QPs can be explicitly differentiated using only the primal solution via a reduced-dimension locally equivalent linear system determined by the active set.
2. We design and implement a modular differentiable layer compatible with any QP solver, enabling plug-and-play flexibility. Our open-source code will be released publicly.
3. We demonstrate state-of-the-art performance in solving and differentiating large-scale, sparse QPs.

2 Related Works

Differentiable Optimization. OptNet [5, 4] differentiates QPs through their optimality conditions, and focuses on small dense problems for GPU batching. They solve the full Jacobian system efficiently by reusing the factorization employed in their custom interior-point method. However, as noted in [17], this comes at the cost of ill-conditioning due to symmetrization. More recent differentiable QP methods include Alt-Diff and SCQPTH [109, 30, 29] which use first-order ADMM and approximately differentiate the fixed point map, and QPLayer [17] which accommodates infeasibility with extended conservative Jacobians. Similarly to OptNet, several of these are tightly integrated with custom algorithms, often to enable access to internal computations required for differentiation. Alt-Diff is coupled with a custom ADMM method, SCQPTH reimplements OSQP, and QPLayer is built on ProxQP. Several works have noticed the importance of the active constraint set in differentiating

constrained optimization problems [8, 57, 89], as well as in the context of quadratic programming [9, 17, 86, 83]. A common observation is that the algebraic system obtained through implicit differentiation can be simplified by removing rows corresponding to inactive constraints. Some works have additionally observed that backpropagation itself can be cast as a distinct equality-constrained QP parameterized by the incoming gradients [8, 86]. However, existing approaches have not used these observations to create a differentiable layer that supports arbitrary black-box QP solvers, missing the opportunity to decouple optimization and differentiation. Other classes of optimization problems, such as convex cone programs [2] and mixed-integer programs [89], have also been differentiated. Some frameworks [1, 24, 92, 39, 96, 22, 90, 102] provide differentiable interfaces to broader classes of optimization problems, but their support of QP has significant limitations. CVXPYLayers [1] reformulates the QP into a cone program to use `diffcp` internally [2] and, as a result, does not support specialized QP solvers, relying exclusively on the cone solvers SCS, ECOS, and Clarabel. The framework Theseus [92] directly handles only unconstrained problems and similarly lacks support for QP-specific solvers. TorchOpt [96] and Optax [39] support unconstrained optimizers used in meta-learning, but require user-defined optimality conditions and user-supplied solvers to handle problems such as QPs. JAXopt [24] includes an implicit differentiation wrapper for CVXPY, which requires symbolic compilation of the QP and does not support sparse matrices; for sparse QPs, JAXopt includes a differentiable re-implementation of OSQP (similar to SCQPTH). Altogether, these drawbacks lead to subpar performance which is reported for some generic methods in previous work on differentiable QPs (e.g., [17]). For completeness, Table 4 in Appendix A summarizes 24 relevant methods, including those discussed above.

Implicit Layers. Optimization layers are a class of implicit layers that use implicit differentiation to compute gradients of solution mappings that lack closed-form expressions [43]. Another class of implicit layer are deep equilibrium models, which are defined by fixed-point mappings and can be interpreted as infinitely deep networks [14, 66, 44, 59, 113, 15]. Similar techniques extend beyond algebraic equations to neural ODEs, where the adjoint state method from parametric PDE control is applied [76, 115, 18, 34]. Implicit differentiation also plays a key role in bi-level programming [36, 72, 56, 3] and meta-learning, where it enables optimization of the outer learning loop [50, 11, 61, 63, 95, 101]. Alternative methods bypass implicit differentiation using approximations – for example, by applying automatic differentiation to iterative algorithms via loop unrolling [19, 20, 81, 105], or by differentiating a single iteration or using Jacobian-free techniques for fixed-point mappings [53, 52, 25].

Sensitivity Analysis and Parametric Programming. There is extensive mathematical theory on the local behavior of optimization problems under perturbations [99, 100], particularly regarding solution sensitivity and stability [47, 49, 48, 73, 26]. While the implicit function theorem is central to this analysis, applying it to optimization problems requires an intermediate step: reformulating the problem through its optimality conditions, which demands several regularity assumptions. Sensitivity theory supports applications such as multi-parametric programming [93], including model predictive control, where problems must often be solved repeatedly for many parameter values, increasing computational costs. To address this, [21] observed that QPs admit closed-form solutions when the active set is known in advance, enabling offline precomputation. The parameter space can be partitioned into regions with fixed active sets [106], where the solution is stable under perturbations. This idea continues to inform modern methods [45, 82, 12].

3 Approach

We begin by formulating the problem, establishing the basic theory of differentiation of QPs, connecting this to our main novel theoretical observation, and concluding with a straightforward algorithm. We note that various subparts of the background we discuss have been used to develop methods for differentiating QPs, see Section 2. However, no single work has fully developed the explicit theory we present or leveraged it to practically implement a fully modular differentiable QP layer.

3.1 Problem Setup: Differentiating QPs

We consider a quadratic program in standard form,

$$\begin{aligned} z^*(\theta) = \arg \min_z \quad & \frac{1}{2} z^T P(\theta) z + q(\theta)^T z \\ \text{s.t.} \quad & A(\theta) z = b(\theta) \\ & C(\theta) z \leq d(\theta), \end{aligned} \tag{1}$$

where $P \in \mathbb{R}^{n \times n}$, $q \in \mathbb{R}^n$, $A \in \mathbb{R}^{p \times n}$, $b \in \mathbb{R}^p$, $C \in \mathbb{R}^{m \times n}$ and $d \in \mathbb{R}^m$ are smoothly parameterized by some $\theta \in \mathbb{R}^s$. We assume that the QP is feasible and strictly convex (*i.e.*, $P \succ 0$). To simplify notation, in the following we omit θ .

This work focuses on computing $\partial_\theta z^*(\theta) = \frac{\partial}{\partial \theta} z^*(\theta)$, the derivative of the optimal point of the QP (1) with respect to the parameters θ . Intuitively, this derivative quantifies the change in the optimal point of the QP in response to a perturbation of its parameters θ . Our goal is to compute $\partial_\theta z^*(\theta)$ *efficiently* and *independently* of the method used to approximate the optimal point $z^*(\theta)$.

An important use case, highlighted in recent work on differentiable optimization, involves incorporating a QP of the form (1) as the ℓ -th layer of a neural network. In this setting, the input to the QP layer, x_ℓ , serves as the parameter vector θ that defines the QP's objective and constraints, and the output is the optimal solution $x_{\ell+1} = z^*(x_\ell)$. Generally, training such a network requires backpropagating gradients through each layer, which involves computing the Jacobian $\frac{\partial x_{\ell+1}}{\partial x_\ell}$. For a QP layer, this Jacobian corresponds to $\partial_\theta z^*(\theta)$, the derivative of the optimal point with respect to the problem parameters. This derivative is also crucial in descent-based methods for solving bi-level optimization problems [36].

3.2 KKT Conditions and Sensitivity Analysis

Our goal is to differentiate QPs using only the solution returned by a black-box numerical solver. To do so, we first establish the necessary theoretical foundations. As is standard in optimization, the required derivatives are obtained via sensitivity analysis of the KKT conditions. This section distills key ideas from optimization theory, sensitivity and parametric analysis, and differentiable programming, framing them in the context of QPs to support the development of dQP.

Optimality Conditions. The first-order Karush–Kuhn–Tucker (KKT) conditions [65, 71, 27, 114] provide a useful algebraic characterization of the optimal points of constrained optimization problems. For the QP (1), the KKT conditions take the form,

$$\begin{aligned} Pz^* + q + A^T \lambda^* + C^T \mu^* &= 0 \\ Az^* - b = 0, \quad Cz^* - d &\leq 0, \quad \mu^* \geq 0 \\ D(\mu^*)(Cz^* - d) &= 0, \end{aligned} \tag{2}$$

where $D(\mu^*) = \text{diag}(\mu^*)$, and the additional variables $\lambda^* \in \mathbb{R}^p$ and $\mu^* \in \mathbb{R}^m$ are the optimal dual variables of the linear equalities and inequalities, respectively. The primal-dual solution of the QP (1) is defined by $\zeta^*(\theta) = (z^*(\theta), \lambda^*(\theta), \mu^*(\theta))$. Under strict convexity and feasibility, the QP (1) has a unique solution $\zeta^*(\theta)$, and the KKT conditions (2) are necessary and sufficient for its optimality.

Active Set and Complementary Slackness. The last equation in (2), the nonlinear complementary slackness condition, plays a central role in our work. Intuitively, it encodes the two possible states of each inequality constraint in (1), $(Cz^* - d)_j \leq 0$. Either (i) the constraint is *active*, meaning it holds with equality $(Cz^* - d)_j = 0$, in which case $\mu_j^* \geq 0$; or (ii) it is *inactive*, satisfied with strict inequality, in which case $\mu_j^* = 0$. Notably, if a constraint is inactive, the same optimal solution z^* would be obtained even if that constraint were removed. We denote the active set by $J(\theta) = \{j : (C(\theta)z^*(\theta) - d(\theta))_j = 0\}$.

Derivatives via Sensitivity Analysis. To differentiate QPs, we apply the Basic Sensitivity Theorem (Theorem 2.1 in [46]), which underpins differentiation of the KKT conditions with respect to θ . Differentiability at θ requires the additional assumption of strict complementary slackness, ruling out the degenerate case where both $(Cz^* - d)_j = 0$ and $\mu_j^* = 0$, thus ensuring that the active set remains unchanged under small perturbations of θ . Under this assumption, the primal-dual

point $\zeta^*(\theta) = (z^*(\theta), \lambda^*(\theta), \mu^*(\theta))$ is differentiable in a neighborhood of θ , optimal for the QP (1), uniquely satisfies the KKT conditions (2), and maintains strict complementary slackness. Crucially, the active set $J(\theta)$ remains fixed in this neighborhood.

With the active set stable, the equality conditions in (2) locally characterize $\zeta(\theta)$. Implicit differentiation of these yields the Jacobians of the solution $\partial_\theta \zeta^*$ in terms of the linear system,

$$\begin{bmatrix} P & A^T & C^T \\ A & 0 & 0 \\ D(\mu^*)C & 0 & D(Cz^* - d) \end{bmatrix} \begin{bmatrix} \partial_\theta z^* \\ \partial_\theta \lambda^* \\ \partial_\theta \mu^* \end{bmatrix} = - \begin{bmatrix} \partial_\theta Pz^* + \partial_\theta q + \partial_\theta A^T \lambda^* + \partial_\theta C^T \mu^* \\ \partial_\theta Az^* - \partial_\theta b \\ D(\mu^*)(\partial_\theta Cz^* - \partial_\theta d) \end{bmatrix}. \quad (3)$$

Under the assumptions of the Basic Sensitivity Theorem, the linear system (3) is invertible. It degenerates exactly in the presence of weakly active constraints $\mu_j^* = (Cz^* - d)_j = 0$, for which the QP is non-differentiable (see, *e.g.*, [5]). For any inactive constraint $j \notin J$, the dual variable μ_j^* vanishes, and thus the corresponding rows and columns of (3) can be removed, yielding the simplified reduced form,

$$\begin{bmatrix} P & A^T & C_J^T \\ A & 0 & 0 \\ C_J & 0 & 0 \end{bmatrix} \begin{bmatrix} \partial_\theta z^* \\ \partial_\theta \lambda^* \\ \partial_\theta \mu_J^* \end{bmatrix} = - \begin{bmatrix} \partial_\theta Pz^* + \partial_\theta q + \partial_\theta A^T \lambda^* + \partial_\theta C_J^T \mu_J^* \\ \partial_\theta Az^* - \partial_\theta b \\ \partial_\theta C_J z^* - \partial_\theta d_J \end{bmatrix}, \quad (4)$$

where μ_J^* , C_J and d_J denote restriction to rows corresponding to active inequality constraints $j \in J$.

3.3 Extracting derivatives from a QP solver’s solution

With the above theory, we derive our main theoretical results and introduce **dQP**, a straightforward algorithm for efficient and robust differentiation of any black-box QP solver.

Our approach stems from two straightforward yet powerful insights: (1) given the *primal* solution of a QP, the active set can be easily identified; (2) once the active set is known, both the primal-dual optimal point and its derivatives can be derived explicitly in closed-form. Furthermore, these quantities can be computed efficiently via a single matrix factorization of a reduced-dimension symmetric system.

These observations lead to a simple algorithm: first, solve the optimization problem using *any* QP solver; then, identify the active set from the solution and solve a linear system to compute the derivatives. Consequently, we can define a “backward pass” for any layer that uses a QP solver, allowing for the seamless integration of any solver best suited to the problem, thus leveraging years of research and development invested in state-of-the-art QP solvers.

Explicit Active Set Differentiation. Consider the QP (1) and its optimal point $\zeta^*(\theta)$, along with the set $J(\theta)$ of active constraints, see Section 3.2. We define the reduced equality-constrained quadratic program, obtained by removing inactive inequalities and converting active inequality constraints into equality constraints,

$$\begin{aligned} z^*(\theta) = \arg \min_z \quad & \frac{1}{2} z^T P(\theta) z + q(\theta)^T z \\ \text{s.t.} \quad & \begin{bmatrix} A(\theta) \\ C(\theta)_{J(\theta)} \end{bmatrix} z = \begin{bmatrix} b(\theta) \\ d(\theta)_{J(\theta)} \end{bmatrix}. \end{aligned} \quad (5)$$

Under the assumptions of Section 3.2, this simpler QP is, in fact, *locally* equivalent to the QP (1), as illustrated in Figure 2. Moreover, it provides an explicit expression for both the primal-dual optimal point and its derivatives:

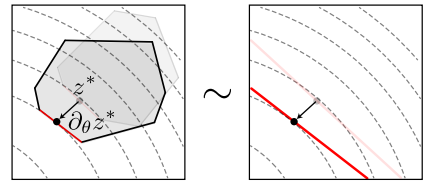


Figure 2: Schematic active set differentiation. Left: a QP is shown by its quadratic level sets and polyhedral feasible set; the solution lies on a facet of the boundary; perturbations of the constraints lead to perturbations in the solution. Right: the perturbation of the solution remains the same when inactive constraints are eliminated.

Theorem 3.1. *The QP (5) is locally equivalent to the reduced equality-constrained QP (1) and its solution $\zeta^*(\theta) = (z^*(\theta), \lambda^*(\theta), \mu^*(\theta))$ admits the explicit form*

$$\begin{bmatrix} z^* \\ \lambda^* \\ \mu_J^* \end{bmatrix} = \begin{bmatrix} P & A^T & C_J^T \\ A & 0 & 0 \\ C_J & 0 & 0 \end{bmatrix}^{-1} \begin{bmatrix} -q \\ b \\ d_J \end{bmatrix}. \quad (6)$$

Furthermore, the optimal point can be explicitly differentiated to obtain

$$\begin{bmatrix} \partial_\theta z^* \\ \partial_\theta \lambda^* \\ \partial_\theta \mu_J^* \end{bmatrix} = \begin{bmatrix} P & A^T & C_J^T \\ A & 0 & 0 \\ C_J & 0 & 0 \end{bmatrix}^{-1} \left(\begin{bmatrix} -\partial_\theta q \\ \partial_\theta b \\ \partial_\theta d_J \end{bmatrix} - \begin{bmatrix} \partial_\theta P & \partial_\theta A^T & \partial_\theta C_J^T \\ \partial_\theta A & 0 & 0 \\ \partial_\theta C_J & 0 & 0 \end{bmatrix} \begin{bmatrix} z^* \\ \lambda^* \\ \mu_J^* \end{bmatrix} \right). \quad (7)$$

A proof of this Theorem, based on the Basic Sensitivity Theorem [46], is provided in Appendix B, along with a calculation of the derivatives using differential matrix calculus [91, 78]. We note that this result is closely related to analyses studied in multi-parametric programming [21, 93, 106, 12, 82].

Explicit differentiation. Notably, for quadratic programming, the Basic Sensitivity Theorem allows us to bypass implicit differentiation techniques [70]. We emphasize that this does not imply that the general solution or its active set admit a closed-form expression. Rather, while we perform explicit differentiation, the implicit function theorem remains key in establishing the local equivalence between the original and reduced problems — the resulting derivatives are the same, though the derivations differ. The derivatives in (7) are obtained via ordinary (explicit) differentiation of the closed-form solution to the reduced QP (6), whereas those in (4) arise from implicit differentiation of the full nonlinear KKT conditions (2), followed by pruning inactive constraints. This distinction, formalized in Theorem 3.1, underscores a critical computational insight: once a black-box solver returns the primal solution, the active set can be identified and the derivatives computed directly via (7). Moreover, if the solver returns only the primal solution, the corresponding dual variables can be recovered using (6). Since both (6) and (7) rely on the same KKT matrix K_J , a single matrix factorization (e.g., via SuperLU [74]) suffices for both steps, adding negligible overhead. These insights culminate in the core algorithm of dQP, summarized in Algorithm 1.

Numerical Computation. Our approach enables compact and efficient gradient computation. The linear system in (7), used to compute both derivatives and dual variables, is symmetric and of reduced size. In contrast, implicit differentiation of the full KKT conditions (1) yields a significantly larger, asymmetric system (3). Beyond simplifying the derivative computation, our approach enables the use of fast, specialized linear solvers that exploit the reduced systems symmetric indefinite KKT matrix structure (e.g., using an LDL factorization as in QDLDL [108, 37]). Empirically, we observe that the reduced linear system (7) is often significantly better conditioned than its full counterpart. Figure 3 illustrates this with an example of a QP governed by two parameters $\theta = (\theta_1, \theta_2)$ of [106], calculated using DAQP [13]. Eliminating inactive constraints improves conditioning significantly.

Figure 3 also highlights a key challenge: computing derivatives near non-differentiable singularities where the active set changes and some constraints become weakly active. In such regions, implicit differentiation becomes severely ill-conditioned. Our method is also affected, primarily through difficulty in determining the correct active set at an approximate solution. Several strategies have been proposed for improving active set identification [33, 84, 28]. Our implementation includes an optional refinement heuristic (Appendix D), though in all our experiments (Section 4), simple hard thresholding of the primal residual $r_j = (Cz^* - d)_j \geq -\epsilon_J$ proved robust.

Implementation. Our open-source implementation will be publicly released. We implement **dQP** (Algorithm 1) as a fully differentiable PyTorch module [88], providing an intuitive interface for integrating differentiable QPs into machine learning and bi-level optimization workflows. The

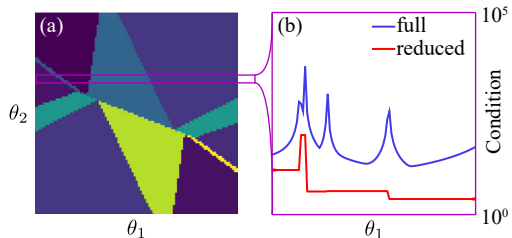


Figure 3: (a) Schematic of active-set parameter space, coloring regions where the active set is constant. (b) Condition number of the full and reduced linear systems along a line in parameter space.

Algorithm 1 – dQP: Differentiation through Black-box Quadratic Programming Solvers

Input: P, q, A, b, C, d , and tolerance ϵ_J
Output: z^*, λ^*, μ^* and $\partial_\theta z^*, \partial_\theta \lambda^*, \partial_\theta \mu^*$

1: Solve QP (1) with any solver for the primal solution z^* (and λ^*, μ^* if available)

2: Compute the active set by thresholding: $J = \{j : (Cz^* - d)_j \geq -\epsilon_J\}$

3: Factorize the reduced KKT system matrix:

$$K_J = \begin{bmatrix} P & A^T & C_J^T \\ A & 0 & 0 \\ C_J & 0 & 0 \end{bmatrix}$$

4: Compute λ^*, μ^* (if not obtained in step (1)):

$$\begin{bmatrix} z^* \\ \lambda^* \\ \mu_J^* \end{bmatrix} = K_J^{-1} \begin{bmatrix} -q \\ b \\ d_J \end{bmatrix}$$

5: Compute the derivatives:

$$\begin{bmatrix} \partial_\theta z^* \\ \partial_\theta \lambda^* \\ \partial_\theta \mu_J^* \end{bmatrix} = K_J^{-1} \left(\begin{bmatrix} -\partial_\theta q \\ \partial_\theta b \\ \partial_\theta d_J \end{bmatrix} - \begin{bmatrix} \partial_\theta P & \partial_\theta A^T & \partial_\theta C_J^T \\ \partial_\theta A & 0 & 0 \\ \partial_\theta C_J & 0 & 0 \end{bmatrix} \begin{bmatrix} z^* \\ \lambda^* \\ \mu_J^* \end{bmatrix} \right)$$

Table 1: Performance of differentiable QP methods for 129 sparse problems from the Maros-Meszaros (MM) dataset [79].

Solver	Full Dataset						Subset of Problems Solved by All Methods					
	# Probs Solved	Avg Fwd [ms]	Avg Bwd [ms]	Avg Total [ms]	Avg Bwd/Total [%]	Accuracy [duality gap]	# Probs Solved	Avg Fwd [ms]	Avg Bwd [ms]	Avg Total [ms]	Avg Bwd/Total [%]	Accuracy [duality gap]
dQP (QPBenchmark)	129	471	996	1467	57%	7.39×10^{-6}	24	10	83	93	35%	1.73×10^{-7}
QPLayer (ProxQP)	77	15089	632	15721	18%	2.21×10^{-2}	24	2828	433	3261	29%	1.77×10^{-4}
OptNet (qpth)	38	39329	2139	41468	6%	2.36×10^{-3}	24	9199	559	9758	7%	1.71×10^{-4}
SCQPTH (OSQP*)	55	16344	6551	22895	13%	1.81×10^{-2}	24	14048	3019	17067	14%	8.75×10^{-3}

implementation supports both dense and sparse problems end-to-end, with appropriate QP and linear solver support. As a PyTorch module, (7) must be rendered as a backward pass; this is described in Appendix C. To ensure modularity, the forward pass supports any QP solver interfaced via the open-source *qp solvers* library [32], which provides lightweight access to over 15 commercial and free open-source solvers and easily supports the integration of new ones. We likewise offer flexibility in the choice of linear solver for differentiation, including support for large-scale sparse solvers like Pardiso [103] and symmetric indefinite solvers like QDLDL [108, 37]. For users unsure of which solver to use, dQP includes a profiling tool to help identify the best-performing QP solver for a given problem. Additional implementation details such as constraint normalization, handling non-differentiability, and warm-starting options for bi-level optimization are discussed in Appendix D.

4 Experimental Results

We have extensively tested dQP to ensure its robustness and evaluate its performance against existing methods for differentiable quadratic programming. Notably, we demonstrate dQP’s strengths in handling large-scale structured and sparse problems, thus complementing custom differentiable GPU-batched solvers such as OptNet [5], which are optimized for solving many small, dense problems simultaneously. Given this focus, and considering the limited availability of state-of-the-art GPU-batchable QP solvers, we conduct our experiments on CPUs, similar to prior works [17, 29, 109, 1]. Our evaluation includes a large benchmark of over 2,000 challenging sparse and dense QPs taken from public and randomly generated problem datasets, designed to test dQPs robustness and performance. Additional experimental details are provided in Appendix E.

Modularity and Performance. We tested dQP on the QP Benchmark suite [31], focusing on 129 large-scale sparse problems from the standard Maros-Meszaros (MM) dataset [79], which are widely used as stress tests for QP solvers. We compared dQP against other differentiable QP methods available in the PyTorch framework: OptNet [5], QPLayer [17], SCQPTH [29], and CVXPYLayers [1]; using the authors’ open-source implementations, each paired with its respective solver. We did not include other general frameworks that either lack direct support for generic QPs in PyTorch, showed subpar performance in our preliminary tests (consistent with findings reported in prior work [17]), or rely on forward passes built on diffcp/CVXPYLayers (see Table 4). For dQP’s forward pass, we selected the top-performing QP solver for each problem, as identified by QP Benchmark [31], to demonstrate the importance of enabling differentiation for the solver that is best suited to each task.

The scatter plot in Figure 4 shows total runtime (forward + backward), duality gap (accuracy), and problem dimension (illustrated by point size) for each differentiable solver and problem. Aggregate performance across the full dataset and the subset of problems solvable by all methods is summarized

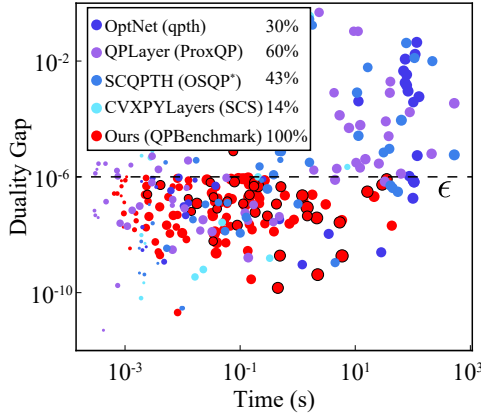


Figure 4: Accuracy versus total forward/backward solve for the Maros-Meszaros dataset [79]. Each point represents a solved problem; point size illustrates dimension; problems solved solely by dQP are circled. The legend shows percentages of success rates; the solvers dQP used and their counts are PIQP 100, Gurobi 9, ProxQP 9, Clarabel 7, OSQP 2, MOSEK 1, QPALM 1.

in Table 1. CVXPYLayers failed on all but 17 small-scale problems and is therefore excluded from the reported statistics. The MM dataset proved especially challenging, with OptNet and SCQPTH solving fewer than 50% of the problems. In contrast, dQP solved all MM problems and was the *only* method to succeed on 38 of them (circled in the figure). Moreover, dQP achieved the best runtime and accuracy in 80% and 78% of all problems, respectively. It performed particularly well on large-scale instances (dimension over 1000), being fastest and most accurate in 97% and 93% of such cases. Additional experiments on 450 random dense QPs and 625 sparse QPs (dimensions 10 to 10^4) are provided in Appendix E.1.3, showing similarly strong performance.

Scalability. We evaluated dQP on large-scale sparse problems that are highly structured, a regime where state-of-the-art QP solvers have a significant advantage over less optimized solvers. Specifically, we tested dQP and other available differentiable QP solvers on two prototypical projection layers expressed as constrained QPs:

$$P_1(x) = \arg \min_z \|x - z\|_2^2 \quad \text{s.t. } 0 \leq z \leq 1, \sum z_i = 1, \quad (8)$$

and

$$P_2(x_1, \dots, x_n) = \arg \min_{z_1, \dots, z_n} \sum \|x_j - z_j\|_2^2 \quad \text{s.t. } \|z_j - z_{j+1}\|_\infty \leq 1. \quad (9)$$

Results for P_1 are shown in Figure 1, demonstrating dQP’s scalability compared to OptNet and QPLayer. Other methods fail on all but small problems (see Appendix E.1.1). In dimensions greater than 2000, dQP outperforms competing methods by 2-3 orders of magnitude in both speed and accuracy. Competing methods are limited to dense calculations and fail in dimensions beyond 10^4 . We note that P_1 is the projection onto the probability simplex, also known as SparseMAX, for

Table 2: Performance analysis for projection onto the probability simplex, formulated in (8). Additional details are provided in Appendix E.1.1 and Table 5.

Solver	Metric	Problem Size						
		20	100	450	1000	4600	10000	100000
dQP (Gurobi)	Accuracy	1.07×10^{-9}	8.88×10^{-10}	2.26×10^{-9}	1.47×10^{-9}	2.72×10^{-9}	9.55×10^{-10}	6.67×10^{-10}
	Time [ms]	1.63	1.92	3.13	5.06	18.46	49.00	476.64
OptNet (qpth)	Accuracy	4.04×10^{-8}	4.24×10^{-8}	1.64×10^{-8}	2.67×10^{-8}	3.95×10^{-8}	6.08×10^{-8}	—
	Time [ms]	2.92	5.19	37.66	182.99	8514.65	70856.43	—
QPLayer (ProxQP)	Accuracy	9.53×10^{-6}	3.65×10^{-5}	4.16×10^{-4}	2.19×10^{-4}	1.16×10^{-3}	1.94×10^{-3}	—
	Time [ms]	0.29	1.61	77.56	751.14	79314.49	946174.68	—
BPQP (OSQP)	Accuracy	2.04×10^{-7}	5.64×10^{-5}	9.66×10^{-4}	3.04×10^{-3}	1.76×10^{-2}	4.02×10^{-2}	—
	Time [ms]	0.32	0.75	5.81	21.68	358.78	1407.05	—
CVXPYLayers (SCS)	Accuracy	1.31×10^{-6}	9.47×10^{-5}	1.31×10^{-3}	2.79×10^{-3}	—	—	—
	Time [ms]	1.97	13.42	156.57	662.60	—	—	—
SCQPTH (OSQP*)	Accuracy	6.19×10^{-7}	—	—	—	—	—	—
	Time [ms]	14.75	—	—	—	—	—	—

Table 3: Performance analysis for projection onto chains, formulated in (9). Additional details are provided in Appendix E.1.2 and Table 6.

Solver	Metric	Problem Size						
		200	500	1000	2000	4000	10000	100000
dQP (Gurobi)	Accuracy	2.73×10^{-7}	2.02×10^{-6}	3.79×10^{-6}	9.16×10^{-6}	2.64×10^{-5}	4.29×10^{-5}	2.81×10^{-4}
dQP (Gurobi)	Time [ms]	6.15	12.99	26.19	47.94	88.35	224.89	2432.64
OptNet (qpth)	Accuracy	6.97×10^{-8}	1.75×10^{-7}	9.22×10^{-8}	2.43×10^{-7}	2.60×10^{-7}	1.98×10^{-7}	—
OptNet (qpth)	Time [ms]	25.38	169.64	907.25	5491.56	34799.98	571710.06	—
QPLayer (ProxQP)	Accuracy	8.46×10^{-5}	8.78×10^{-5}	1.82×10^{-4}	2.97×10^{-4}	6.95×10^{-4}	1.03×10^{-3}	—
QPLayer (ProxQP)	Time [ms]	8.04	81.93	577.11	3996.92	30748.67	471649.91	—
SCQPTH (OSQP [*])	Accuracy	1.67×10^{-5}	2.83×10^{-5}	4.76×10^{-5}	6.64×10^{-5}	7.80×10^{-5}	1.21×10^{-4}	—
SCQPTH (OSQP [*])	Time [ms]	13.20	67.55	407.13	2755.28	16628.15	195462.18	—
CVXPYLayers (SCS)	Accuracy	1.69×10^{-1}	2.18×10^{-1}	2.97×10^{-1}	—	—	—	—
CVXPYLayers (SCS)	Time [ms]	129.26	683.34	2048.34	—	—	—	—

which more efficient, non-QP-based methods exist [80]. Results for P_2 , representing projection onto “chains” with bounded links, exhibit similar scalability and are detailed in Appendix E.1.2.

Bi-Level Geometry Optimization. We further demonstrate the scalability of our approach on a bi-level optimization problem introduced in [69]:

$$\begin{aligned} M^* = \arg \min_M \| \mu^*(M) \|_2^2 \\ \text{s.t. } (v^*(M), \lambda^*(M), \mu^*(M)) = \arg \min_v \{ \text{tr}(v^T M v) \text{ s.t. } Bv = u, Cv \succeq 0 \}. \end{aligned} \quad (10)$$

In this problem $v \in \mathbb{R}^{n \times 2}$ represents the n vertex coordinates of a triangular mesh, $M \in \mathbb{R}^{n \times n}$ is a parameterized Laplacian, and B , u and C encode boundary conditions. $\mu^*(M)$ is the dual variable corresponding to linear inequalities of the lower-level problem. The results described in [69] imply that if $\mu^*(M)$ vanishes then $v^*(M^*)$, at the optimal Laplacian M^* , represents a straight-edge intersection-free drawing of the mesh [112]. The solution to (10) is visualized in Figure 5(a) for an example large-scale ant mesh. Additionally, Figure 5(b) shows that dQP scales more favorably with problem size compared to OptNet, QPLayer and SCQPTH; in particular, only dQP supports problems with over 10^4 vertices.

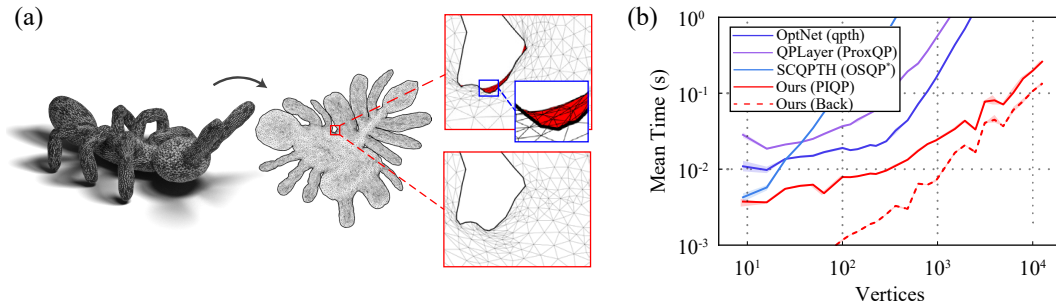


Figure 5: (a) Planar embedding of a large-scale ant mesh (15k vertices). Zoom-ins show: (top) a non-injective harmonic map with edge overlaps highlighted in red; (bottom) dQP’s injective solution to the bi-level problem (10). (b) Scalability: solver runtimes as mesh size increases for a synthetic problem.

5 Conclusion

We introduce the dQP framework for differentiating QPs by leveraging the local equivalence between a QP and a simpler equality-constrained problem. dQP provides a straightforward differentiable interface for any QP solver, yielding an efficient QP layer that can be readily integrated into neural architectures, among other applications. We note that our current method does not yet support full parallelization or GPU acceleration, as state-of-the-art sparse and scalable QP solvers with GPU support are still lacking. We recognize these as important challenges and limitations to address in future work. We see the present work as an important step toward developing similar solver-agnostic differentiable layers for other popular optimization problems (*e.g.*, semidefinite programming), which we plan to explore in future research.

References

- [1] Agrawal, A., Amos, B., Barratt, S., Boyd, S., Diamond, S., and Kolter, J. Z. Differentiable convex optimization layers. In *Advances in Neural Information Processing Systems*, 2019.
- [2] Agrawal, A., Barratt, S., Boyd, S., Busseti, E., and Moursi, W. M. Differentiating through a cone program. *Journal of Applied and Numerical Optimization*, 1(2):107–115, 2019.
- [3] Alesiani, F. Implicit bilevel optimization: Differentiating through bilevel optimization programming. In *Proceedings of the AAAI Conference on Artificial Intelligence*, volume 37, pp. 14683–14691, 2023.
- [4] Amos, B. Differentiable optimization-based modeling for machine learning. *Ph.D. Thesis*, 2019.
- [5] Amos, B. and Kolter, J. Z. Optnet: Differentiable optimization as a layer in neural networks. In *International conference on machine learning*, pp. 136–145. PMLR, 2017.
- [6] Amos, B. and Kolter, J. Z. qpth-cvxpyp. <https://github.com/locuslab/qpth/blob/master/qpth/solvers/cvxpyp.py>, 2017.
- [7] Amos, B. and Kolter, J. Z. qpth-sparse. <https://github.com/locuslab/qpth/blob/master/qpth/solvers/pdipm/spbatch.py>, 2017.
- [8] Amos, B., Xu, L., and Kolter, J. Z. Input convex neural networks. In Precup, D. and Teh, Y. W. (eds.), *Proceedings of the 34th International Conference on Machine Learning*, volume 70 of *Proceedings of Machine Learning Research*, pp. 146–155. PMLR, 06–11 Aug 2017.
- [9] Amos, B., Jimenez, I., Sacks, J., Boots, B., and Kolter, J. Z. Differentiable mpc for end-to-end planning and control. In Bengio, S., Wallach, H., Larochelle, H., Grauman, K., Cesa-Bianchi, N., and Garnett, R. (eds.), *Advances in Neural Information Processing Systems*, volume 31. Curran Associates, Inc., 2018.
- [10] Andersen, E. D. and Andersen, K. D. The mosek interior point optimizer for linear programming: an implementation of the homogeneous algorithm. In *High performance optimization*, pp. 197–232. Springer, 2000.
- [11] Andrychowicz, M., Denil, M., Gomez, S., Hoffman, M. W., Pfau, D., Schaul, T., Shillingford, B., and De Freitas, N. Learning to learn by gradient descent by gradient descent. *Advances in neural information processing systems*, 29, 2016.
- [12] Arnström, D. and Axehill, D. A high-performant multi-parametric quadratic programming solver, 2024.
- [13] Arnström, D., Bemporad, A., and Axehill, D. A dual active-set solver for embedded quadratic programming using recursive LDL^T updates. *IEEE Transactions on Automatic Control*, 67(8):4362–4369, 2022.
- [14] Bai, S., Kolter, J. Z., and Koltun, V. Deep equilibrium models. In Wallach, H., Larochelle, H., Beygelzimer, A., d'Alché-Buc, F., Fox, E., and Garnett, R. (eds.), *Advances in Neural Information Processing Systems*, volume 32. Curran Associates, Inc., 2019.
- [15] Bai, S., Koltun, V., and Kolter, J. Z. Multiscale deep equilibrium models. In Larochelle, H., Ranzato, M., Hadsell, R., Balcan, M., and Lin, H. (eds.), *Advances in Neural Information Processing Systems*, volume 33, pp. 5238–5250. Curran Associates, Inc., 2020.
- [16] Bambade, A., Schramm, F., El Kazdadi, S., Caron, S., Taylor, A. B., and Carpentier, J. Proxqp: an efficient and versatile quadratic programming solver for real-time robotics applications and beyond. 2023.
- [17] Bambade, A., Schramm, F., Taylor, A. B., and Carpentier, J. Leveraging augmented-lagrangian techniques for differentiating over infeasible quadratic programs in machine learning. In *The Twelfth International Conference on Learning Representations, ICLR 2024, Vienna, Austria, May 7-11, 2024*. OpenReview.net, 2024.

- [18] Beatson, A., Ash, J. T., Roeder, G., Xue, T., and Adams, R. P. Learning composable energy surrogates for pde order reduction. In *Proceedings of the 34th International Conference on Neural Information Processing Systems, NIPS '20*, Red Hook, NY, USA, 2020. Curran Associates Inc. ISBN 9781713829546.
- [19] Belanger, D. and McCallum, A. Structured prediction energy networks. In *International Conference on Machine Learning*, pp. 983–992. PMLR, 2016.
- [20] Belanger, D., Yang, B., and McCallum, A. End-to-end learning for structured prediction energy networks. In *International Conference on Machine Learning*, pp. 429–439. PMLR, 2017.
- [21] Bemporad, A., Morari, M., Dua, V., and Pistikopoulos, E. N. The explicit linear quadratic regulator for constrained systems. *Automatica*, 38(1):3–20, 2002. ISSN 0005-1098.
- [22] Besançon, M., Dias Garcia, J., Legat, B., and Sharma, A. Flexible differentiable optimization via model transformations. *INFORMS Journal on Computing*, 36(2):456–478, 2024.
- [23] Blondel, M. and Roulet, V. The elements of differentiable programming. *arXiv preprint arXiv:2403.14606*, 2024.
- [24] Blondel, M., Berthet, Q., Cuturi, M., Frostig, R., Hoyer, S., Llinares-López, F., Pedregosa, F., and Vert, J.-P. Efficient and modular implicit differentiation. *Advances in neural information processing systems*, 35:5230–5242, 2022.
- [25] Bolte, J., Pauwels, E., and Vaiter, S. One-step differentiation of iterative algorithms. In *Thirty-seventh Conference on Neural Information Processing Systems*, 2023.
- [26] Bonnans, J. F. and Shapiro, A. *Perturbation analysis of optimization problems*. Springer Science & Business Media, 2013.
- [27] Boyd, S. and Vandenberghe, L. *Convex optimization*. Cambridge university press, 2004.
- [28] Burke, J. V. and Moré, J. J. On the identification of active constraints. *SIAM Journal on Numerical Analysis*, 25(5):1197–1211, 1988. ISSN 00361429.
- [29] Butler, A. Scqpth: an efficient differentiable splitting method for convex quadratic programming. 08 2023.
- [30] Butler, A. and Kwon, R. H. Efficient differentiable quadratic programming layers: an admm approach. *Computational Optimization and Applications*, 84(2):449–476, 2023.
- [31] Caron, S., Zaki, A., Otta, P., Arnström, D., Carpentier, J., Yang, F., and Leziart, P.-A. qpbenchmark: Benchmark for quadratic programming solvers available in Python. <https://github.com/qpsolvers/qpbenchmark>, 2024.
- [32] Caron, S. et al. QPSOLVERS: Quadratic Programming Solvers in Python. <https://github.com/qpsolvers/qpsolvers>, March 2024.
- [33] Cartis, C. and Yan, Y. Active-set prediction for interior point methods using controlled perturbations. *Computational Optimization and Applications*, 63(3):639–684, Apr 2016. ISSN 1573-2894.
- [34] Chen, R. T. Q., Rubanova, Y., Bettencourt, J., and Duvenaud, D. K. Neural ordinary differential equations. In Bengio, S., Wallach, H., Larochelle, H., Grauman, K., Cesa-Bianchi, N., and Garnett, R. (eds.), *Advances in Neural Information Processing Systems*, volume 31. Curran Associates, Inc., 2018.
- [35] Chen, R. T. Q., Amos, B., and Nickel, M. Semi-discrete normalizing flows through differentiable voronoi tessellation. In *ICLR Workshop on Deep Generative Models for Highly Structured Data*, 2022.
- [36] Colson, B., Marcotte, P., and Savard, G. An overview of bilevel optimization. *Annals of operations research*, 153:235–256, 2007.

[37] Davis, T. A. Algorithm 849: A concise sparse cholesky factorization package. *ACM Transactions on Mathematical Software (TOMS)*, 31(4):587–591, 2005.

[38] de Avila Belbute-Peres, F., Smith, K., Allen, K., Tenenbaum, J., and Kolter, J. Z. End-to-end differentiable physics for learning and control. In Bengio, S., Wallach, H., Larochelle, H., Grauman, K., Cesa-Bianchi, N., and Garnett, R. (eds.), *Advances in Neural Information Processing Systems*, volume 31. Curran Associates, Inc., 2018.

[39] DeepMind, Babuschkin, I., Baumli, K., Bell, A., Bhupatiraju, S., Bruce, J., Buchlovsky, P., Budden, D., Cai, T., Clark, A., Danihelka, I., Dedieu, A., Fantacci, C., Godwin, J., Jones, C., Hemsley, R., Hennigan, T., Hessel, M., Hou, S., Kapturowski, S., Keck, T., Kemaev, I., King, M., Kunesch, M., Martens, L., Merzic, H., Mikulik, V., Norman, T., Papamakarios, G., Quan, J., Ring, R., Ruiz, F., Sanchez, A., Sartran, L., Schneider, R., Sezener, E., Spencer, S., Srinivasan, S., Stanojević, M., Stokowiec, W., Wang, L., Zhou, G., and Viola, F. The DeepMind JAX Ecosystem, 2020. URL <http://github.com/google-deepmind>.

[40] Ding, S., Wang, J., Du, Y., and Shi, Y. Reduced policy optimization for continuous control with hard constraints. In *Proceedings of the 37th International Conference on Neural Information Processing Systems*, NIPS '23, Red Hook, NY, USA, 2024. Curran Associates Inc.

[41] Du, X., Aigerman, N., Zhou, Q., Kovalsky, S. Z., Yan, Y., Kaufman, D. M., and Ju, T. Lifting simplices to find injectivity. *ACM Transactions on Graphics*, 39(4), 2020.

[42] Dunning, I., Huchette, J., and Lubin, M. Jump: A modeling language for mathematical optimization. *SIAM Review*, 59(2):295–320, 2017. doi: 10.1137/15M1020575.

[43] Duvenaud, D., Kolter, J. Z., and Johnson, M. Deep implicit layers tutorial-neural odes, deep equilibrium models, and beyond. *Neural Information Processing Systems Tutorial*, 2020.

[44] El Ghaoui, L., Gu, F., Travacca, B., Askari, A., and Tsai, A. Implicit deep learning. *SIAM Journal on Mathematics of Data Science*, 3(3):930–958, 2021.

[45] Ferreau, H. J., Kirches, C., Potschka, A., Bock, H. G., and Diehl, M. qpoases: A parametric active-set algorithm for quadratic programming. *Mathematical Programming Computation*, 6: 327–363, 2014.

[46] Fiacco, A. V. Sensitivity analysis for nonlinear programming using penalty methods. *Mathematical Programming*, 10(1):287–311, Dec 1976. ISSN 1436-4646.

[47] Fiacco, A. V. *Introduction to sensitivity and stability analysis in non linear programming*. New York: Academic Press, 1983.

[48] Fiacco, A. V. and McCormick, G. P. *Nonlinear programming: sequential unconstrained minimization techniques*. John Wiley & Sons, New York, NY, USA, 1968. Reprinted by SIAM Publications in 1990.

[49] Fiacco, Anthony V. and Ishizuka, Y. Sensitivity and stability analysis for nonlinear programming. *Annals of Operations Research*, 27(1):215–235, 1990.

[50] Finn, C. B. *Learning to learn with gradients*. University of California, Berkeley, 2018.

[51] Frison, G. and Diehl, M. Hpmipm: a high-performance quadratic programming framework for model predictive control**this research was supported by the german federal ministry for economic affairs and energy (bmwi) via eco4wind (0324125b) and dyconpv (0324166b), and by dfg via research unit for 2401. *IFAC-PapersOnLine*, 53(2):6563–6569, 2020. ISSN 2405-8963. 21st IFAC World Congress.

[52] Fung, S. W., Heaton, H., Li, Q., McKenzie, D., Osher, S. J., and Yin, W. JFB: jacobian-free backpropagation for implicit networks. In *Thirty-Sixth AAAI Conference on Artificial Intelligence, AAAI 2022, Thirty-Fourth Conference on Innovative Applications of Artificial Intelligence, IAAI 2022, The Twelfth Symposium on Educational Advances in Artificial Intelligence, EAAI 2022 Virtual Event, February 22 - March 1, 2022*, pp. 6648–6656. AAAI Press, 2022.

[53] Geng, Z., Zhang, X.-Y., Bai, S., Wang, Y., and Lin, Z. On training implicit models. In Beygelzimer, A., Dauphin, Y., Liang, P., and Vaughan, J. W. (eds.), *Advances in Neural Information Processing Systems*, 2021.

[54] Goldfarb, D. and Idnani, A. A numerically stable dual method for solving strictly convex quadratic programs. *Mathematical Programming*, 27(1):1–33, Sep 1983. ISSN 1436-4646.

[55] Goulart, P. J. and Chen, Y. Clarabel: An interior-point solver for conic programs with quadratic objectives, 2024.

[56] Gould, S., Fernando, B., Cherian, A., Anderson, P., Cruz, R. S., and Guo, E. On differentiating parameterized argmin and argmax problems with application to bi-level optimization. *arXiv preprint arXiv:1607.05447*, 2016.

[57] Gould, S., Hartley, R., and Campbell, D. Deep declarative networks. *IEEE Transactions on Pattern Analysis and Machine Intelligence*, 44(8):3988–4004, 2022.

[58] Gurobi Optimization, LLC. Gurobi Optimizer Reference Manual, 2024.

[59] Gurumurthy, S., Bai, S., Manchester, Z., and Kolter, J. Z. Joint inference and input optimization in equilibrium networks. *Advances in Neural Information Processing Systems*, 34:16818–16832, 2021.

[60] Hermans, B., Themelis, A., and Patrinos, P. QPALM: A Newton-type Proximal Augmented Lagrangian Method for Quadratic Programs. In *58th IEEE Conference on Decision and Control*, Dec. 2019.

[61] Hochreiter, S., Younger, A. S., and Conwell, P. R. Learning to learn using gradient descent. In *Artificial Neural Networks—ICANN 2001: International Conference Vienna, Austria, August 21–25, 2001 Proceedings 11*, pp. 87–94. Springer, 2001.

[62] Holmes, C., Dümbgen, F., and Barfoot, T. D. Sdprlayers: Certifiable backpropagation through polynomial optimization problems in robotics, 2024.

[63] Hospedales, T., Antoniou, A., Micaelli, P., and Storkey, A. Meta-learning in neural networks: A survey. *IEEE transactions on pattern analysis and machine intelligence*, 44(9):5149–5169, 2021.

[64] Huangfu, Q. and Hall, J. A. J. Parallelizing the dual revised simplex method. *Mathematical Programming Computation*, 10(1):119–142, Mar 2018. ISSN 1867-2957.

[65] Karush, W. Minima of functions of several variables with inequalities as side constraints. Master’s thesis, Department of Mathematics, University of Chicago, 1939.

[66] Kawaguchi, K. On the theory of implicit deep learning: Global convergence with implicit layers. In *International Conference on Learning Representations*, 2021.

[67] Kingma, D. P. and Ba, J. Adam: A method for stochastic optimization, 2017.

[68] Kovalsky, S. Z., Glasner, D., and Basri, R. A global approach for solving edge-matching puzzles. *SIAM Journal on Imaging Sciences*, 8(2):916–938, 2015.

[69] Kovalsky, S. Z., Aigerman, N., Daubechies, I., Kazhdan, M., Lu, J., and Steinerberger, S. Non-convex planar harmonic maps. *arXiv preprint arXiv:2001.01322*, 2020.

[70] Krantz, S. G. and Parks, H. R. *The Implicit Function Theorem*. Birkhäuser Boston, MA, 2012.

[71] Kuhn, H. W. and Tucker, A. W. Nonlinear programming. In Neyman, J. (ed.), *Proceedings of the Second Berkeley Symposium on Mathematical Statistics and Probability*, pp. 481–492. University of California Press, 1951.

[72] Kunisch, K. and Pock, T. A bilevel optimization approach for parameter learning in variational models. *SIAM Journal on Imaging Sciences*, 6(2):938–983, 2013.

[73] Lee, G., Tam, N., and Nguyen, D. Y. Quadratic programming and affine variational inequalities, a qualitative study. *Springer New York, NY*, 01 2010.

[74] Li, X. S. An overview of superlu: Algorithms, implementation, and user interface. *ACM Trans. Math. Softw.*, 31(3):302–325, September 2005. ISSN 0098-3500.

[75] Ling, C. K., Fang, F., and Kolter, J. Z. What game are we playing? end-to-end learning in normal and extensive form games. *arXiv preprint arXiv:1805.02777*, 2018.

[76] Lions, J.-L. *Optimal control of systems governed by partial differential equations*. Springer-Verlag, Berlin, 1971. ISBN 3340051155. Translation of Contrôle optimal de systèmes gouvernés par des équations aux dérivées partielles.

[77] Liu, Z., Liu, L., Wang, X., and Zhao, P. DFWLayer: Differentiable frank-wolfe optimization layer. In *The Second Tiny Papers Track at ICLR 2024*, 2024.

[78] Magnus, J. R. and Neudecker, H. *Matrix Differential Calculus*. New York, 1988.

[79] Maros, I. and Mészáros, C. A repository of convex quadratic programming problems. *Optimization methods and software*, 11(1-4):671–681, 1999.

[80] Martins, A. and Astudillo, R. From softmax to sparsemax: A sparse model of attention and multi-label classification. In Balcan, M. F. and Weinberger, K. Q. (eds.), *Proceedings of The 33rd International Conference on Machine Learning*, volume 48 of *Proceedings of Machine Learning Research*, pp. 1614–1623, New York, New York, USA, 20–22 Jun 2016. PMLR.

[81] Metz, L., Maheswaranathan, N., Nixon, J., Freeman, D., and Sohl-Dickstein, J. Understanding and correcting pathologies in the training of learned optimizers. In *International Conference on Machine Learning*, pp. 4556–4565. PMLR, 2019.

[82] Narciso, D. A., Pappas, I., Martins, F., and Pistikopoulos, E. N. A new solution strategy for multiparametric quadratic programming. *Computers & Chemical Engineering*, 164:107882, 2022. ISSN 0098-1354.

[83] Niculae, V., Martins, A., Blondel, M., and Cardie, C. SparseMAP: Differentiable sparse structured inference. In Dy, J. and Krause, A. (eds.), *Proceedings of the 35th International Conference on Machine Learning*, volume 80 of *Proceedings of Machine Learning Research*, pp. 3799–3808. PMLR, 10–15 Jul 2018.

[84] Oberlin, C. and Wright, S. J. Active set identification in nonlinear programming. *SIAM Journal on Optimization*, 17(2):577–29, 2006. Copyright - Copyright] © 2006 Society for Industrial and Applied Mathematics; Last updated - 2023-12-04.

[85] O’Donoghue, B., Chu, E., Parikh, N., and Boyd, S. Conic optimization via operator splitting and homogeneous self-dual embedding. *Journal of Optimization Theory and Applications*, 169(3):1042–1068, 2016.

[86] Pan, J., Ye, Z., Yang, X., Yang, X., Liu, W., Wang, L., and Bian, J. BPQP: A differentiable convex optimization framework for efficient end-to-end learning. In *The Thirty-eighth Annual Conference on Neural Information Processing Systems*, 2024. URL <https://openreview.net/forum?id=VKKY3Uv7vi>.

[87] Pandala, A. G., Ding, Y., and Park, H.-W. qpswift: A real-time sparse quadratic program solver for robotic applications. *IEEE Robotics and Automation Letters*, 4(4):3355–3362, 2019.

[88] Paszke, A. et al. *PyTorch: an imperative style, high-performance deep learning library*. Curran Associates Inc., Red Hook, NY, USA, 2019.

[89] Paulus, A., Rolinek, M., Musil, V., Amos, B., and Martius, G. Comboptnet: Fit the right np-hard problem by learning integer programming constraints. In Meila, M. and Zhang, T. (eds.), *Proceedings of the 38th International Conference on Machine Learning*, volume 139 of *Proceedings of Machine Learning Research*, pp. 8443–8453. PMLR, 18–24 Jul 2021.

[90] Paulus, A., Martius, G., and Musil, V. LPGD: A general framework for backpropagation through embedded optimization layers. In Salakhutdinov, R., Kolter, Z., Heller, K., Weller, A., Oliver, N., Scarlett, J., and Berkenkamp, F. (eds.), *Proceedings of the 41st International Conference on Machine Learning*, volume 235 of *Proceedings of Machine Learning Research*, pp. 39989–40014. PMLR, 21–27 Jul 2024.

[91] Petersen, K. B. and Pedersen, M. S. The matrix cookbook. *Technical University of Denmark*, 7(15):510, 2008.

[92] Pineda, L., Fan, T., Monge, M., Venkataraman, S., Sodhi, P., Chen, R. T. Q., Ortiz, J., DeTone, D., Wang, A., Anderson, S., Dong, J., Amos, B., and Mukadam, M. Theseus: A library for differentiable nonlinear optimization. In Koyejo, S., Mohamed, S., Agarwal, A., Belgrave, D., Cho, K., and Oh, A. (eds.), *Advances in Neural Information Processing Systems*, volume 35, pp. 3801–3818. Curran Associates, Inc., 2022.

[93] Pistikopoulos, E. N., Diangelakis, N. A., and Oberdieck, R. *Multi-parametric optimization and control*. John Wiley & Sons, 2020.

[94] Pogančić, M. V., Paulus, A., Musil, V., Martius, G., and Rolinek, M. Differentiation of blackbox combinatorial solvers. In *International Conference on Learning Representations*, 2020.

[95] Rajeswaran, A., Finn, C., Kakade, S. M., and Levine, S. Meta-learning with implicit gradients. *Advances in neural information processing systems*, 32, 2019.

[96] Ren*, J., Feng*, X., Liu*, B., Pan*, X., Fu, Y., Mai, L., and Yang, Y. Torchopt: An efficient library for differentiable optimization. *Journal of Machine Learning Research*, 24(367):1–14, 2023.

[97] Rezende, D. J. and Racanière, S. Implicit riemannian concave potential maps, 2021.

[98] Richter-Powell, J., Lorraine, J., and Amos, B. Input convex gradient networks. *arXiv preprint arXiv:2111.12187*, 2021.

[99] Rockafellar, R. T. *Convex Analysis*. Princeton University Press, Princeton, 1970. ISBN 9781400873173.

[100] Rockafellar, R. T. and Wets, R. *Variational Analysis*, volume 317. Springer Berlin, Heidelberg, 01 1998. ISBN 978-3-540-62772-2.

[101] Sambharya, R., Hall, G., Amos, B., and Stellato, B. Learning to warm-start fixed-point optimization algorithms. *Journal of Machine Learning Research*, 25(166):1–46, 2024.

[102] Schaller, M. and Boyd, S. Code generation for solving and differentiating through convex optimization problems, 2025.

[103] Schenk, O. and Gärtner, K. Solving unsymmetric sparse systems of linear equations with pardiso. *Future Generation Computer Systems*, 20(3):475–487, 2004.

[104] Schwan, R., Jiang, Y., Kuhn, D., and Jones, C. N. PIQP: A proximal interior-point quadratic programming solver. In *2023 62nd IEEE Conference on Decision and Control (CDC)*, pp. 1088–1093, 2023.

[105] Scieur, D., Gidel, G., Bertrand, Q., and Pedregosa, F. The curse of unrolling: Rate of differentiating through optimization. In Oh, A. H., Agarwal, A., Belgrave, D., and Cho, K. (eds.), *Advances in Neural Information Processing Systems*, 2022.

[106] Spjøtvold, J., Kerrigan, E. C., Jones, C. N., Tøndel, P., and Johansen, T. A. On the facet-to-facet property of solutions to convex parametric quadratic programs. *Automatica*, 42(12): 2209–2214, 2006. ISSN 0005-1098.

[107] Stellato, B. and O’Donoghue, B. Osqph: A c interface to qldl for parametric qp solvers. <https://github.com/osqp/osqph>, 2023.

- [108] Stellato, B., Banjac, G., Goulart, P., Bemporad, A., and Boyd, S. OSQP: an operator splitting solver for quadratic programs. *Mathematical Programming Computation*, 12(4):637–672, 2020.
- [109] Sun, H., Shi, Y., Wang, J., Tuan, H. D., Poor, H. V., and Tao, D. Alternating differentiation for optimization layers. *arXiv preprint arXiv:2210.01802*, 2022.
- [110] Tan, Y., Terekhov, D., and Delong, A. Learning linear programs from optimal decisions. In Larochelle, H., Ranzato, M., Hadsell, R., Balcan, M., and Lin, H. (eds.), *Advances in Neural Information Processing Systems*, volume 33, pp. 19738–19749. Curran Associates, Inc., 2020.
- [111] Thayaparan, M., Valentino, M., Ferreira, D., Rozanova, J., and Freitas, A. Diff-explainer: Differentiable convex optimization for explainable multi-hop inference. *Transactions of the Association for Computational Linguistics*, 10:1103–1119, 2022.
- [112] Tutte, W. T. How to draw a graph. *Proceedings of the London Mathematical Society*, 3(1):743–767, 1963.
- [113] Winston, E. and Kolter, J. Z. Monotone operator equilibrium networks. In Larochelle, H., Ranzato, M., Hadsell, R., Balcan, M., and Lin, H. (eds.), *Advances in Neural Information Processing Systems*, volume 33, pp. 10718–10728. Curran Associates, Inc., 2020.
- [114] Wright, S. J. Numerical optimization, 2006.
- [115] Xue, T., Beatson, A., Adriaenssens, S., and Adams, R. Amortized finite element analysis for fast PDE-constrained optimization. In III, H. D. and Singh, A. (eds.), *Proceedings of the 37th International Conference on Machine Learning*, volume 119 of *Proceedings of Machine Learning Research*, pp. 10638–10647. PMLR, 13–18 Jul 2020.
- [116] Zhang, H., Nguyen, D. H., and Tsuda, K. Differentiable optimization layers enhance gnn-based mitosis detection. *Scientific Reports*, 13(1):14306, 2023.

A Existing Methods for Differentiable Optimization

Table 4 provides an overview of existing differentiable optimization methods for quadratic programming (QP), more general conic programs (CP) and other optimization problems.

Table 4: Comparison of differentiable optimization libraries and layers.

Name	Programs	Solvers	Features	Limitations
OptNet [5]	QP	qpth	GPU batchable. Re-uses factorization from forward for fast backward solve.	Solver specific. Sparsity not supported.
QPLayer [17]	QP	ProxQP	Supports infeasible QPs. Tightly couples to ProxQP.	Solver specific. Sparsity not supported.
SCQPTH [29]	QP	OSQP	Differentiates ADMM updates. Supports infeasibility detection and automatic scaling.	Solver specific. Sparsity not supported.
Diffcp [2]	CP	SCS, ECOS, Clarabel	Supports sparse cone programs (CP).	Supports specific conic solvers.
CVXPYLayers [1]	CP	diffcp	Flexible problem formulation and solver choice. Supports sparsity.	Inherits diffcp limitations.
BPQP [86]	QP, SOCP	OSQP	Computes derivatives by solving a second equality-constrained QP.	Published implementation is incomplete.
Alt-Diff [109]	QP	Custom ADMM	Differentiates ADMM updates. Supports inexact solutions.	Reportedly slow [17].
LQP [30]	QP	Custom ADMM		Box constraints only.
LPGD [90]	CP	diffcp	Modifies diffcp to handle degenerate derivatives.	Inherits diffcp limitations.
CVXPYgen [102]	QP, SOCP	OSQP	Accelerates CVXPYlayers by C compilation of problem formulation.	Solver specific.
JAXopt-general [24]	User supplied	User supplied	Differentiates arbitrary implicit functions.	User must manually provide KKT..
JAXopt-OSQP [24]	QP	Custom GPU OSQP	GPU batchable.	Solver specific.
JAXopt-CVXPYQP [24]	QP	CVXPY	Flexible problem formulation and solver choice.	Inherits CVXPY limitations. Sparsity not supported.
SDPRLayers [62]	CP	CVXPY	Flexible problem formulation and solver choice.	Inherits CVXPY limitations.
Torchopt [96]	User supplied	User supplied	Differentiates arbitrary implicit functions.	User must manually provide KKT.
Optax [39]	Specialized	Specialized		Supports specialized problems/solvers, e.g., projections.
DiffOpt.jl [22]	Various	JuMP-supported solvers [42]	Supports a variety of convex and non-convex problems.	JuMP provides QP support only for COSMO, OSQP, and Ipopt
Theseus [92]	NLS	CHOLMOD, cudaLU, BaSpach	Supports non-linear least squares (NLS). GPU batchable. Supports sparsity.	Lacks hard constraints.
OptNet-Sparse [7]	QP	qpth		Published implementation is incomplete.
OptNet-CVXPY [6]	QP	CVXPY		Published implementation is incomplete.
OSQPTH [107]	QP	OSQP		Published implementation is incomplete.
DFWLLayer [77]	QP	Frank-Wolfe	Automatically differentiates an unrolled Frank-Wolfe solver.	Solver specific.
CombOptNet [89]	ILP	Gurobi	Differentiation of combinatorial solvers	
Blackbox-Backprop [94]	MIP	Gurobi MIP, Blossom V, Dijkstra	Differentiation of combinatorial solvers	

Remarks. This table includes all relevant differentiable optimization methods known to us at the time of writing. In some cases, code was available online without an associated publication. Among all listed methods that directly support generic QP without modification, only dQP, QPLayer, SDPRLayers, and DiffOpt.jl return both the dual optimal point of a QP and its derivatives. Notably, dQP is the sole QP method that supports a wide variety of solvers with minimal-overhead through *qpsolvers*, in contrast to a significant number of methods that build on top of CVXPY/CVXPYLayers, which requires a compilation step (e.g., SDPRLayers, JAXopt-CVXPYQP, OptNet-CVXPY) and/or diffcp which has limited solvers compared to ordinary, non-differentiable CVXPY (e.g., LPGD). Several methods are available only outside the PyTorch framework (e.g., JAXopt, Optax, DiffOpt.jl).

B Proof of Theorem 1

In this section we provide a proof of Theorem 1, which we restate below:

Theorem B.1. *The QP (5) is locally equivalent to the reduced equality-constrained QP (1) and its solution $\zeta^*(\theta) = (z^*(\theta), \lambda^*(\theta), \mu^*(\theta))$ admits the explicit form*

$$\begin{bmatrix} z^* \\ \lambda^* \\ \mu_J^* \end{bmatrix} = \begin{bmatrix} P & A^T & C_J^T \\ A & 0 & 0 \\ C_J & 0 & 0 \end{bmatrix}^{-1} \begin{bmatrix} -q \\ b \\ d_J \end{bmatrix}. \quad (11)$$

Furthermore, the optimal point can be explicitly differentiated to obtain

$$\begin{bmatrix} \partial_\theta z^* \\ \partial_\theta \lambda^* \\ \partial_\theta \mu_J^* \end{bmatrix} = - \begin{bmatrix} P & A^T & C_J^T \\ A & 0 & 0 \\ C_J & 0 & 0 \end{bmatrix}^{-1} \left(\begin{bmatrix} \partial_\theta P & \partial_\theta A^T & \partial_\theta C_J^T \\ \partial_\theta A & 0 & 0 \\ \partial_\theta C_J & 0 & 0 \end{bmatrix} \begin{bmatrix} z^* \\ \lambda^* \\ \mu_J^* \end{bmatrix} - \begin{bmatrix} -\partial_\theta q \\ \partial_\theta b \\ \partial_\theta d_J \end{bmatrix} \right). \quad (12)$$

Proof. We begin by establishing that the QP (1) and the equality-constrained reduced QP (5) are equivalent. For any θ satisfying the assumptions of the theorem, the QP (1) has a unique solution characterized by the KKT system

$$\begin{aligned} P(\theta)z^*(\theta) + q(\theta) + A(\theta)^T \lambda^*(\theta) + C(\theta)^T \mu^*(\theta) &= 0 \\ A(\theta)z^*(\theta) - b(\theta) &= 0 \\ C(\theta)z^*(\theta) - d(\theta) &\leq 0 \\ \mu^*(\theta) &\geq 0 \\ D(\mu^*(\theta))(C(\theta)z^*(\theta) - d(\theta)) &= 0. \end{aligned} \quad (13)$$

Complementarity implies that active constraints $j \in J(\theta)$ have $\mu^*(\theta)_j > 0$ and therefore must be satisfied with an equality $(C(\theta)z^*(\theta) - d(\theta))_j = 0$, while inactive constraints $j \notin J(\theta)$ have $\mu^*(\theta)_j = 0$ and thus can be eliminated, without altering the solution. Therefore, the unique solution $\zeta^*(\theta) = (z^*(\theta), \lambda^*(\theta), \mu^*(\theta))$ of (13) is also the unique solution of the reduced system

$$\begin{aligned} P(\theta)z^*(\theta) + q(\theta) + A(\theta)^T \lambda^*(\theta) + C(\theta)_{J(\theta)}^T \mu^*(\theta)_{J(\theta)} &= 0 \\ A(\theta)z^*(\theta) - b(\theta) &= 0 \\ C(\theta)_{J(\theta)}z^*(\theta) - d(\theta)_{J(\theta)} &= 0, \end{aligned} \quad (14)$$

which are exactly the KKT conditions of the equality-constrained reduced QP (5). Uniqueness of solution then implies that (1) and (5) are pointwise equivalent at θ . Moreover, since P, q, A, b, C, d are smoothly parameterized by θ , the Basic Sensitivity Theorem [46] asserts that the primal-dual solution $\zeta^*(\theta)$ for (1) is a differentiable function of θ in a neighborhood of θ , defined implicitly through the KKT's equality conditions. Furthermore, the active set $J(\theta)$ is fixed in this neighborhood, therefore (1) and (5) are locally equivalent.

(14) implies that the reduced primal-dual solution $\zeta_J^*(\theta) = (z^*(\theta), \lambda^*(\theta), \mu_J^*(\theta))$ satisfies $K_J(\theta)\zeta_J^*(\theta) = v_J(\theta)$, where

$$K_J(\theta) = \begin{bmatrix} P(\theta) & A(\theta)^T & C(\theta)_{J(\theta)}^T \\ A(\theta) & 0 & 0 \\ C(\theta)_{J(\theta)} & 0 & 0 \end{bmatrix}, \quad v_J(\theta) = \begin{bmatrix} -q(\theta) \\ b(\theta) \\ d(\theta)_{J(\theta)} \end{bmatrix}. \quad (15)$$

Under the assumptions of the theorem, the reduced KKT matrix $K_J(\theta)$ is invertible and

$$\zeta_J^* = K_J^{-1}v_J, \quad (16)$$

yielding (6). Moreover, since $J(\theta)$ is locally constant, the Basic Sensitivity Theorem establishes that $\zeta_J^*(\theta)$ is differentiable. Using the formal derivative of the matrix inverse [78, 91] we *explicitly* differentiate (16) to obtain

$$\partial_\theta \zeta_J^* = (-K_J^{-1}(\partial_\theta K)K_J^{-1})v_J + K_J^{-1}(\partial_\theta v_J) = -K_J^{-1}(\partial_\theta K_J)\zeta_J^* + K_J^{-1}(\partial_\theta v_J), \quad (17)$$

yielding (7). \square

C Backpropagation

Like other differentiable QP layers implemented within automatic differentiation frameworks such as PyTorch [88], we do not directly return the derivative $\partial_\theta \zeta^*$. This is in part because dQP directly receives the QP parameters P, q, A, b, C, d and not θ , and so in backpropagation we are not concerned with θ . This is rather accounted for in the next step outside dQP, usually by automatic differentiation. Secondly, backpropagation requires that we compute a so-called Jacobian-vector product which are products of the Jacobians with an “incoming” gradient of a quantity or loss ℓ that depends on ζ^* . This requires less computation and does not require the formation of a 3-tensor. Since $\zeta_J^* = K_J^{-1}v_J$ is a formal matrix-vector multiplication, the Jacobian-vector product is well-known,

$$\nabla_{v_J} \ell = (K_J^{-1})^T \nabla_{\zeta_J^*} \ell, \quad (18)$$

and

$$\nabla_{K_J} \ell = -\nabla_{v_J} \ell \zeta_J^{*T}, \quad (19)$$

with respect to K_J, v_J , respectively. Although backpropagation introduces a transposition, the re-use of a factorization from solving for the active duals is unaffected. This follows from the symmetry of the reduced KKT matrix which simplifies (18) into $\nabla_{v_J} \ell = K_J^{-1} \nabla_{\zeta_J^*} \ell$. Next, we extract the gradients with respect to the parameters by the chain rule. This amounts to tracking their position in the blocks and accounting for symmetry constraints. It is helpful to write $(d_z, d_\lambda, d_{\mu_J}) = -\nabla_{v_J} \ell$ so that we express

$$\begin{aligned} \nabla_P \ell &= \frac{1}{2} (d_z z^{*T} + z^* d_z^T) & \nabla_q \ell &= d_z \\ \nabla_A \ell &= d_\lambda z^{*T} + \lambda^* d_z^T & \nabla_b \ell &= -d_\lambda \\ \nabla_C \ell &= d_{\mu_J} z^{*T} + \mu_J^* d_z^T & \nabla_{d_J} \ell &= -d_{\mu_J}, \end{aligned} \quad (20)$$

similar to OptNet [5]. We note that the gradient with respect to P is constrained to lie within the subspace of symmetric matrices. Similarly, if the matrices P, A, C are sparse, then we project the gradient to lie within the non-zero entries, which can be implemented efficiently in Equations 20. Although the above argument is for a scalar loss ℓ , the same approach is naturally adapted if ζ^* is mapped to a vector in the immediate next layer.

D Implementation Details

Choosing a solver. Since our work enables users to choose any QP solver as the front-end for their differentiable QP applications, we include a simple diagnostic tool for quantitatively measuring solver performance. We present an example result in Figure 6 for the cross geometry experiment in section 4, finding PIQP, OSQP, and QPALM to be the most efficient. For this reason, we choose PIQP in the geometry experiments. We also include tools for checking the solution and gradient accuracy.

Tolerances. In addition to the active set tolerance ϵ_J , QP solvers often support additional user-provided tolerances. These include the primal residual which measures violations of feasibility, the dual residual which measures violations of stationarity, and for some solvers also the duality gap, which provides a direct handle on solution accuracy. We inherit the structure of *qpsolvers* for setting custom tolerances on different QP solvers, though we set a heuristic default which is sufficient for many of the experiments in this work.

Convexity and Feasibility. Two key assumptions of our method are strict convexity and feasibility. However, these are often violated in practice. We include optional checks that P is symmetric positive definite. On the other hand, we do not perform any special handling for infeasibility – a limitation of our method compared to, for example, QPLayer [17].

Non-differentiable Points. For non-differentiable problems, we solve for the derivatives in the least-squares sense, plugging the system into *qpsolvers* which can handle least-squares, or a standard least-squares solver. We attempt to anticipate weakly active constraints which cause non-differentiability by measuring the norms of the primal residual and the dual. Additionally, the reduced KKT is non-invertible if the active dual solution is not unique and so we check a necessary condition: the total number of active constraints plus the number of equalities must be less than the dimension. If these checks are passed, we attempt the standard linear solve and pass to least-squares if it fails.

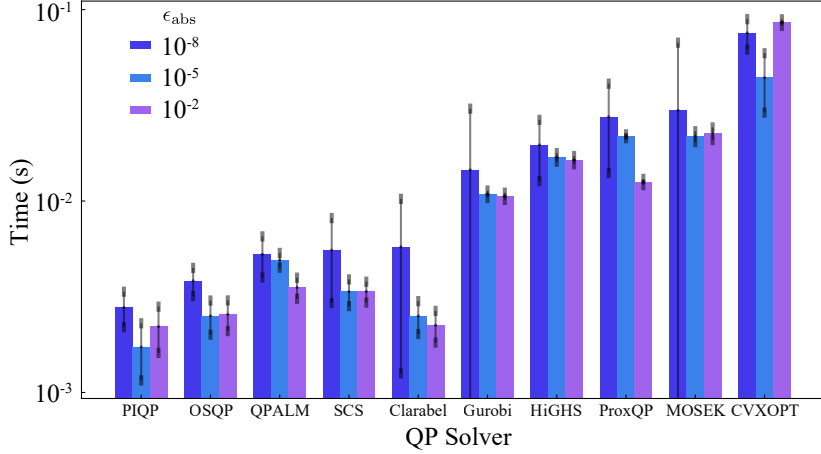


Figure 6: Evaluating the best QP solver for the cross geometry problem using our diagnostic tool. The solution tolerance regimes are varied between $\epsilon_{\text{abs}} = 10^{-8}, 10^{-5}, 10^{-2}$.

Normalization. Some problems have large variations in scale between different rows within the constraints. This influences the primal residual and thus the active set, which is determined by comparing with an absolute threshold tolerance. To address this issue for these problems, we include an *optional* differentiable normalization step on the constraints before Algorithm 1 is carried out. Under this choice, the resulting relative primal residual becomes the scale-invariant distance to the constraint.

Equality Constraints. While we include equality constraints in our general formulation, they are not required.

Warm-Start. Since *qpsolvers* supports warm-starting, we inherit it as an option and store data in the PyTorch module from previous outer iterations, which can be used as initialization. This is useful for bi-level optimization problems where the input θ changes little between outer iterations. We did not use this feature in our bi-level optimization experiment.

Fixed Parameters. For fixed parameters, we do not compute the corresponding derivative. This saves the cost of unwrapping the linear solve as in (20) and saves the memory to form the loss gradients, which are matrices for P, A, C .

Active Set Refinement. Inaccuracy in a solution may lead to instability in the active set near weakly active constraints, degrading the gradient quality. To show this, we repeat the experiment in Figure 3 which has a simple polyhedral active set parameter space. One setup where instability appears is illustrated in Figure 7 where we use absolute solver tolerance $\epsilon_{\text{abs}} = 10^{-4}$ and a much tighter active tolerance $\epsilon_J = 10^{-7}$. Qualitatively, the active set at each solution is severely degraded, even for points away from the boundaries where the set changes. We provide a *optional* heuristic algorithm

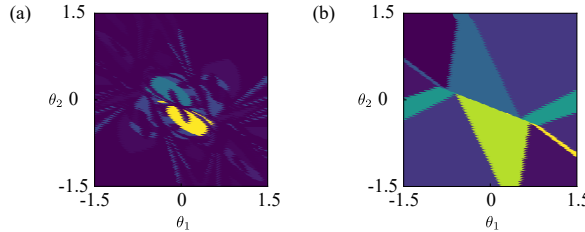


Figure 7: The set-up in figure 3 with looser solver tolerance $\epsilon_{\text{abs}} = 10^{-4}$, active tolerance $\epsilon_J = 10^{-7}$, and solver PIQP. (a) The computed active set is degraded due to the inaccurate solution. (b) Our heuristic active set refinement algorithm recovers the ground truth active sets.

to address this, which recovers the desired set in this problem. First, we order the constraints by increasing residual and select an initial active set from the tolerance ϵ_J . Then, we progressively add

constraints by checking if the residual of the system 6 for ζ_J^* decreases, and greedily accepting until adding constraints no longer improves the residual. At each step, we keep the primal solution from the forward fixed, and solve for the new active dual variables. While this algorithm works well on simple examples, more sophisticated and efficient techniques may be desired for harder problems. We did not use this refinement algorithm in any of our experiments.

QP Solvers. Throughout this work, we use a number of QP solvers available in *qpsolvers* including Clarabel [55], DAQP [13], Gurobi [58], HiGHS [64], HPIPM [51], MOSEK [10], OSQP [108], PIQP [104], ProxQP [16], QPALM [60], qpSWIFT [87], quadprog [54], and SCS [85].

E Experimental Details

For completeness and reproducibility, we include additional details on the experiments. We run all experiments and methods on CPU, including methods that support GPU such as OptNet.

E.1 Performance Evaluation

All experiments in this section were run on a Macbook Air with Apple M2 chips, 8 cores, and 16GB RAM.

In our QP benchmark experiments, we evaluate the solution accuracy using the primal residual r_p (the maximum error on equality and inequality constraints), dual residual r_d (the maximum error on the dual feasibility condition), and duality gap r_g (the difference between primal and dual optimal values).

$$\begin{aligned} r_p &= \max(\|Az - b\|_\infty, [Cz - d]_+) \\ r_d &= \|Pz + q + A^T \lambda + C^T \mu\|_\infty \\ r_g &= |z^T Pz + q^T z + b^T \lambda + d^T \mu| \end{aligned}$$

Throughout our experiments, we present results for the duality gap to indicate the solution accuracy since, for a strongly convex QP, a zero duality gap $r_g = 0$ is a necessary and sufficient condition for optimality.

For the forward, we set the absolute residual tolerance to $\epsilon_{\text{abs}} = 10^{-6}$ and the active constraint tolerance to $\epsilon_J = 10^{-5}$. We run each problem separately with batch size 1.

In our benchmark, we regard a problem as successfully solved if it meets the following criteria:

1. The solve time is less than a practical 800s time limit.
2. The primal residual, dual residual, and duality gap are less than 1.0. This is a coarse check, less stringent than the imposed tolerances.
3. The differentiation is executed, and does not lead to a fatal error (e.g. due to non-invertibility of a linear system).

Experimental results are averaged over 5 independent samples.

Since SCQPTH does not support equality constraints, we convert them into an corresponding set of inequality constraints.

E.1.1 Projection onto the probability simplex

For projection onto the probability simplex, as formulated in P_1 , equation (8), we set $x \in \mathbb{R}^n$ with $x_i \sim \mathcal{N}(0, 1)$. The dataset, with 500 problems, has dimensions $n \in \{10, 20, 50, 100, 220, 450, 1000, 2100, 4600, 10000, 100000\}$. For $n \leq 4600$, each dimension contains 50 problems and 25 problems for $n > 4600$. Gurobi is chosen as dQP's forward solver. Figure 1 shows the median performance within the 1/4 and 3/4 quantiles for each dimension. SCQPTH failed for all problems with $n > 50$. The statistics in Table 5 show that we outperform competing methods for differentiable QP in both forward and backward times.

Table 5: Time and accuracy performance statistics for projection onto the probability simplex.

Solver	Metric	Problem Size						
		20	100	450	1000	4600	10000	100000
dQP (Gurobi)	Accuracy	1.07×10^{-9}	8.88×10^{-10}	2.26×10^{-9}	1.47×10^{-9}	2.72×10^{-9}	9.55×10^{-10}	6.67×10^{-10}
	Forward [ms]	1.38	1.65	2.66	4.37	15.83	42.21	423.91
	Backward [ms]	0.24	0.28	0.46	0.69	2.58	6.21	53.45
	Total [ms]	1.63	1.92	3.13	5.06	18.46	49.00	476.64
OptNet (qpth)	Accuracy	4.04×10^{-8}	4.24×10^{-8}	1.64×10^{-8}	2.67×10^{-8}	3.95×10^{-8}	6.08×10^{-8}	Failed
	Forward [ms]	2.72	4.72	33.46	165.50	7788.73	65976.45	—
	Backward [ms]	0.20	0.46	3.99	17.48	720.43	4958.74	—
	Total [ms]	2.92	5.19	37.66	182.99	8514.65	70856.43	—
QPLayer (ProxQP)	Accuracy	9.53×10^{-6}	3.65×10^{-5}	4.16×10^{-4}	2.19×10^{-4}	1.16×10^{-3}	1.94×10^{-3}	Failed
	Forward [ms]	0.14	1.23	66.73	657.88	71724.25	869532.53	—
	Backward [ms]	0.14	0.37	10.85	91.72	7594.93	77831.58	—
	Total [ms]	0.29	1.61	77.56	751.14	79314.49	946174.68	—
BPQP (OSQP)	Accuracy	2.04×10^{-7}	5.64×10^{-5}	9.66×10^{-4}	3.04×10^{-3}	1.76×10^{-2}	4.02×10^{-2}	Failed
	Forward [ms]	0.11	0.40	3.88	14.45	226.27	712.20	—
	Backward [ms]	0.21	0.34	1.90	7.10	132.73	692.37	—
	Total [ms]	0.32	0.75	5.81	21.68	358.78	1407.05	—
CVXPYLayers (SCS)	Accuracy	1.31×10^{-6}	9.47×10^{-5}	1.31×10^{-3}	2.79×10^{-3}	Failed	Failed	Failed
	Forward [ms]	1.30	10.51	131.60	537.26	—	—	—
	Backward [ms]	0.66	2.92	23.83	123.25	—	—	—
	Total [ms]	1.97	13.42	156.57	662.60	—	—	—
SCQPTH (OSQP*)	Accuracy	6.19×10^{-7}	Failed	Failed	Failed	Failed	Failed	Failed
	Forward [ms]	14.35	—	—	—	—	—	—
	Backward [ms]	0.40	—	—	—	—	—	—
	Total [ms]	14.75	—	—	—	—	—	—

Table 6: Time and accuracy performance statistics for projection onto chains.

Solver	Metric	Problem Size						
		200	500	1000	2000	4000	10000	100000
dQP (Gurobi)	Accuracy	2.73×10^{-7}	2.02×10^{-6}	3.79×10^{-6}	9.16×10^{-6}	2.64×10^{-5}	4.29×10^{-5}	2.81×10^{-4}
	Forward [ms]	5.66	12.04	24.41	44.79	82.57	209.79	2263.54
	Backward [ms]	0.49	0.98	1.74	3.18	5.81	14.69	172.80
	Total [ms]	6.15	12.99	26.19	47.94	88.35	224.89	2432.64
OptNet (qpth)	Accuracy	6.97×10^{-8}	1.75×10^{-7}	9.22×10^{-8}	2.43×10^{-7}	2.60×10^{-7}	1.98×10^{-7}	Failed
	Forward [ms]	23.37	156.49	845.24	5124.87	32528.54	536702.00	—
	Backward [ms]	1.98	13.06	61.41	365.02	2266.20	35438.33	—
	Total [ms]	25.38	169.64	907.25	5491.56	34799.98	571710.06	—
QPLayer (ProxQP)	Accuracy	8.46×10^{-5}	8.78×10^{-5}	1.82×10^{-4}	2.97×10^{-4}	6.95×10^{-4}	1.03×10^{-3}	Failed
	Forward [ms]	6.60	69.90	505.05	3484.47	26921.57	414295.22	—
	Backward [ms]	1.44	12.10	72.13	512.95	3833.25	57219.68	—
	Total [ms]	8.04	81.93	577.11	3996.92	30748.67	471649.91	—
SCQPTH (OSQP*)	Accuracy	1.67×10^{-5}	2.83×10^{-5}	4.76×10^{-5}	6.64×10^{-5}	7.80×10^{-5}	1.21×10^{-4}	Failed
	Forward [ms]	10.02	39.49	236.61	1617.88	8258.89	65507.05	—
	Backward [ms]	3.17	28.46	170.88	1126.46	8374.37	129385.97	—
	Total [ms]	13.20	67.55	407.13	2755.28	16628.15	195462.18	—
CVXPYLayers (SCS)	Accuracy	1.69×10^{-1}	2.18×10^{-1}	2.97×10^{-1}	Failed	Failed	Failed	Failed
	Forward [ms]	94.70	510.04	1644.47	—	—	—	—
	Backward [ms]	36.27	167.21	404.12	—	—	—	—
	Total [ms]	129.26	683.34	2048.34	—	—	—	—

E.1.2 Projection onto chain

For projection onto chains with links of length bounded by 1 in ∞ -norm, as formulated in P_2 , equation (9), the input point cloud $x_1, \dots, x_m \in \mathbb{R}^d$ is set with $x_i \sim \mathcal{N}(0, 100I_d)$, where the number of points is $m = 100$. By varying the dimension of the vector, d , we generated a 300 problem dataset with dimensions $n \in \{200, 500, 1000, 2000, 4000, 10000, 100000\}$. For $n \leq 4000$, each dimension contains 50 problems; for $n > 4000$ each dimension contains 25 problems. Gurobi is chosen as dQP's forward solver. Figure 8 and Table 6 demonstrate the solvers have performance similar to the projection onto the probability simplex shown in Figure 1, in terms of efficiency. Additionally, dQP successfully solves large-scale problems that other solvers fail to solve.

E.1.3 Random sparse/dense problems

We generated two datasets of random QPs: sparse and dense.

For the random sparse dataset, $P = L^T L$, where L is the standard Laplacian matrix of k -nearest graph ($k = 3$). Entries of C and A are filled by $\mathcal{N}(0, 1)$ random numbers with density of 5×10^{-4} ; entirely zero rows are avoided. The vectors d and b are generated so that the constraints are feasible $d = C\mathbf{1} + \mathbf{1}$ and $b = A\mathbf{1}$. The dataset contains 625 problems with dimensions spanning $n \in \{100, 220, 450, 1000, 2100, 4600, 10000\}$, where $m = n$ and $p = n/2$. For $n \leq 4600$, each dimension contains 100 problems; for $n > 4600$ each dimension contains 25 problems. The KKT

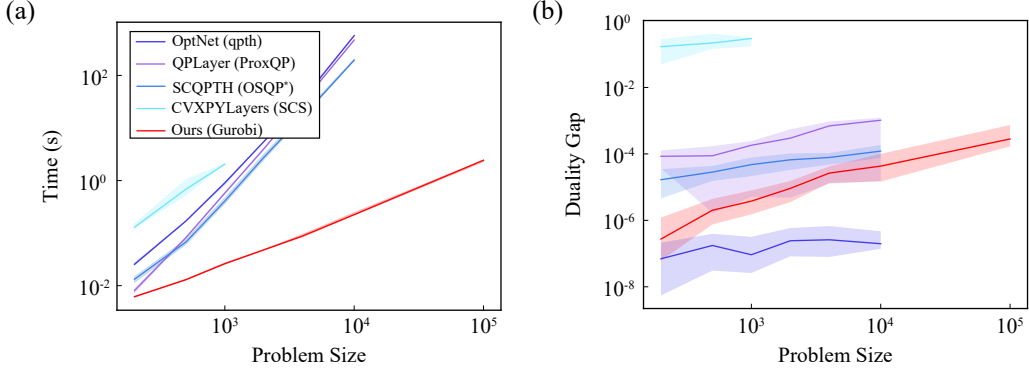


Figure 8: Time and accuracy performance for projection onto chains.

systems in these problems tend to be ill-conditioned. We use Gurobi as dQP’s forward solver and employ a least-squares solver for the backward. In our experiments, shown in Table 7, OptNet and CVXPYLayers fail on all problems and SCQPTH is substantially slower, failing for $n \geq 4600$. dQP demonstrates superior accuracy and efficiency over QPLayer.

For the random dense dataset, $P = Q^T Q + 10^{-4} I$, where $Q \in \mathbb{R}^{n \times n}$ with $Q_{ij} \sim \mathcal{U}(0, 1)$, $C \in \mathbb{R}^{m \times n}$ with $C_{ij} \sim \mathcal{U}(0, 1)$, and $A \in \mathbb{R}^{p \times n}$ with $A_{ij} \sim \mathcal{U}(0, 1)$. The constraint vectors are chosen in the same way as the sparse case. The dataset contains 450 problems with dimensions spanning $n \in \{10, 20, 50, 100, 220, 450, 1000, 2100, 4600\}$, $m = n$, and $p = n/2$. Each dimension contains 50 problems. We use DAQP and ProxQP as dQP’s forward solvers. In the regime of these dense problems, qpth and ProxQP—the forward solvers used by OptNet and QPLayer, respectively—are highly competitive with other available solvers, both free and commercial. As such, we do not expect dQP to yield substantial gains. Indeed, Table 8 shows that our method is comparable to OptNet and QPLayer in both runtime and accuracy. For smaller dimensions ($n \leq 1000$), DAQP offers higher accuracy, while for larger problems, ProxQP proves more efficient.

Table 7: Time and accuracy performance statistics on random sparse problems.

Solver	Metric	Problem Size						
		100	220	450	1000	2100	4600	10000
dQP (Gurobi)	Accuracy	4.46×10^{-8}	9.23×10^{-8}	1.34×10^{-7}	6.89×10^{-7}	1.34×10^{-6}	3.16×10^{-6}	3.43×10^{-6}
	Forward [ms]	2.57	3.44	5.53	11.07	60.68	2446.70	143209.89
	Backward [ms]	1.79	2.86	4.73	9.70	24.03	309.10	9364.61
	Total [ms]	4.37	6.33	10.28	20.72	90.01	2760.07	151471.27
OptNet (qpth)		Failed						
QPLayer (ProxQP)	Accuracy	6.46×10^{-6}	1.25×10^{-5}	1.69×10^{-5}	3.04×10^{-5}	6.12×10^{-5}	1.77×10^{-3}	7.82×10^{-5}
	Forward [ms]	1.04	5.47	31.11	235.00	2268.24	23597.22	199009.91
	Backward [ms]	0.30	1.17	7.46	51.00	393.68	3538.53	38466.29
	Total [ms]	1.34	6.63	38.56	285.99	2658.82	27133.19	240084.62
SCQPTH (OSQP*)	Accuracy	2.21×10^{-7}	3.96×10^{-7}	1.64×10^{-6}	2.85×10^{-5}	1.32×10^{-1}	Failed	Failed
	Forward [ms]	4.43	8.36	27.64	4153.39	79627.33	-	-
	Backward [ms]	1.37	4.92	25.99	177.81	1588.04	-	-
	Total [ms]	5.82	13.38	53.84	4331.38	81211.59	-	-
CVXPYLayers (SCS)		Failed						

E.2 Bi-Level Geometry Optimization

The geometry experiments were run on an Intel(R) Core(TM) i7-8850H CPU @ 2.60GHz with 6 cores.

We include a supplementary example in Figure 9 which illustrates the boundary conditions (inequality constraints in (10)) of [68] using blue arrows (corresponding to applying the Laplacian to the output vertices) and cones at points where the shape is locally non-convex. If the arrows fall outside the cones as shown in (b), then the map is non-invertible; if instead they lie strictly inside the cones then the map is invertible as shown in (c). The process is also flexible: by adding a regularizing term $\lambda \left\| \frac{M}{\|M\|_F} - \frac{M_c}{\|M_c\|_F} \right\|_\infty$ that measures the distance to the combinatorial Laplacian M_c shown in (d),

Table 8: Time and accuracy performance statistics on random dense problems.

Solver	Metric	Problem Size					
		20	100	450	1000	2100	4600
dQP (daqp)	Accuracy	1.59×10^{-11}	1.20×10^{-8}	2.35×10^{-6}	4.08×10^{-5}	5.26×10^{-4}	Failed
	Forward [ms]	0.20	1.31	131.35	1115.62	10065.77	-
	Backward [ms]	0.14	0.48	11.22	56.90	313.90	-
	Total [ms]	0.34	1.81	144.91	1174.47	10379.68	-
dQP (proxqp)	Accuracy	4.71×10^{-6}	6.42×10^{-5}	9.11×10^{-4}	7.26×10^{-4}	4.13×10^{-4}	4.25×10^{-4}
	Forward [ms]	0.29	2.54	61.12	379.74	2553.82	26408.12
	Backward [ms]	0.17	1.85	13.53	70.25	385.04	3369.77
	Total [ms]	0.46	4.32	73.68	455.22	2935.93	29771.33
OptNet (qpth)	Accuracy	6.89×10^{-8}	2.51×10^{-8}	3.80×10^{-8}	3.51×10^{-7}	2.80×10^{-6}	3.34×10^{-5}
	Forward [ms]	2.99	7.09	78.56	463.04	3176.59	29387.34
	Backward [ms]	0.23	0.45	5.55	29.30	185.80	1540.07
	Total [ms]	3.22	7.56	84.20	491.57	3362.25	30931.00
QPLayer (ProxQP)	Accuracy	3.08×10^{-6}	6.88×10^{-5}	3.98×10^{-5}	1.31×10^{-4}	1.35×10^{-5}	1.48×10^{-4}
	Forward [ms]	0.14	0.99	43.11	407.77	3973.89	43740.91
	Backward [ms]	0.15	0.34	9.67	74.24	601.25	5781.58
	Total [ms]	0.29	1.35	52.99	482.17	4575.13	49558.44
SCQPTH (OSQP*)	Accuracy	3.48×10^{-5}	4.62×10^{-4}	4.32×10^{-5}	6.54×10^{-5}	1.83×10^{-4}	2.26×10^{-3}
	Forward [ms]	10.01	26.72	120.12	664.74	6802.36	384565.40
	Backward [ms]	0.47	1.28	26.80	184.22	1733.72	15203.05
	Total [ms]	10.50	27.90	147.25	850.37	8550.04	399699.87
CVXPYLayers (SCS)	Accuracy	5.40×10^{-4}	Failed	Failed	Failed	Failed	Failed
	Forward [ms]	3.15	-	-	-	-	-
	Backward [ms]	1.08	-	-	-	-	-
	Total [ms]	4.22	-	-	-	-	-

we can enhance map quality in the sense that the triangles change their shape less with respect to the input mesh (a).

The upper-level loss for the bi-level cross experiment is shown in Figure 10(a) where the unregularized loss is driven to the desired tolerance, accompanied by sudden changes in the active set as the dual variables are driven to zero. We terminate the optimization at convergence, once all constraints are inactive to guarantee an injective map. For the regularized optimization (Figure 10(b)), we choose the regularization hyper-parameter to be $\lambda = 10$ after sample testing. Despite the regularization, the dual loss can still be driven to 0 to reach an injective map.

To optimize over Laplacians M , we directly parameterize the space of Laplacians; we impose that the diagonals are the absolute row sums during optimization and that the off-diagonals are negative. We also constrain M to have the same sparsity pattern as the combinatorial Laplacian. Lastly, since the Laplacian M is the quadratic term in 1 the resulting QP is not strictly convex because the Laplacian does not have strictly positive eigenvalues. To address this, we perturb M by a small scaling of the identity $10^{-4}I$.

Throughout the geometry experiments, we use the same solution tolerance $\epsilon_{\text{abs}} = 10^{-5}$ and active tolerance $\epsilon_J = 10^{-4}$ with the forward solver PIQP as determined by our tool for choosing the best solver described in Appendix D. For the upper-level optimization, we use the Adam optimizer with learning rate 10^{-2} [67]. We initialize the bi-level optimization with M_c .

We report only forward (QP) time for OptNet, QPLayer and SCQPTH in Figure 5(b) because OptNet and SCQPTH do not output, nor differentiate the duals, and while QPLayer does, it suffers poor scaling from dense operations. The backward timing that we report for dQP excludes any contribution coming from the set-up of the parameterized Laplacian and directly report the time to solve the reduced KKT and extract the gradients with respect to M .

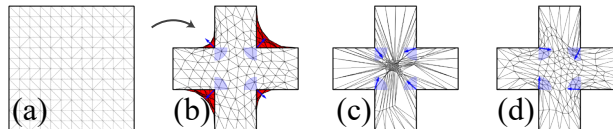


Figure 9: Computing an invertible map into a non-convex plus sign. A naive mapping from (a) the square into (b) the plus without cone constraints has inversions (red). Including cone constraints (blue) and performing the bi-level optimization leads to (c) an invertible map which can be regularized to (d) an enhanced quality map.

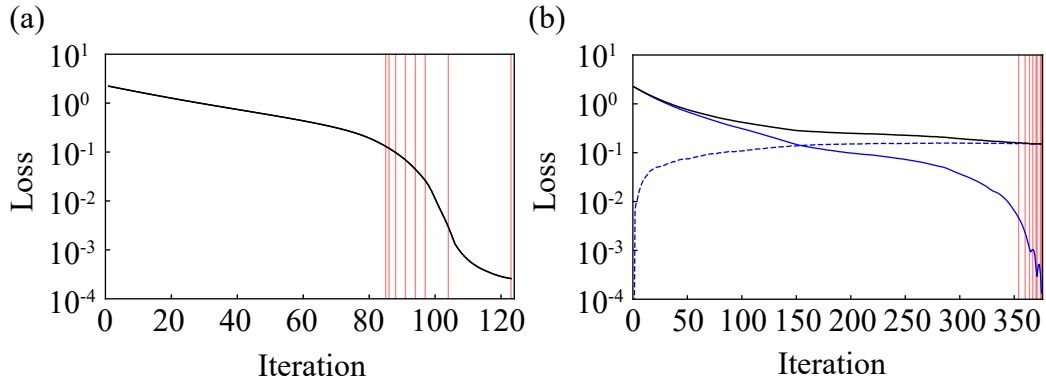


Figure 10: The evolution of the loss for the mappings of the square into the cross. Iterations for which the active set changes are denoted with vertical red lines. (a) Without regularization, the loss is driven monotonically to the tolerance. (b) With a competing regularizing loss term (dashed), convergence to the tolerance is slowed but not prevented.

The cross (Figure 9) and ant (Figure 5(a)) meshes and boundary constraints are obtained from the datasets in [41]. We create the synthetic mesh refinement example in Figure 5(b) by perturbing the corner of a square mesh.